

N70-19861

BOEING

DOCUMENT NO. D6-29356TN

OPTIMIZATION OF DUCT LININGS FOR SOUND ATTENUATION

MODEL Research/Contract

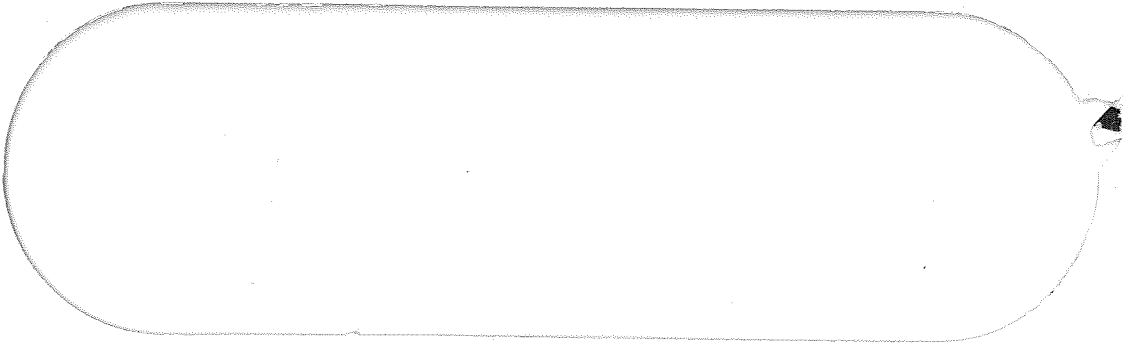
Distribution of this document is unlimited;
it may be released to the general public.

J D C
RECEIVED
~~JAN 24 1972~~
REGULATED
B

**CASE FILE
COPY**

DISTRIBUTION STATEMENT A

Approved for public release;
Distribution Unlimited



ACCESSION for

CFSTI WHITE SECTION

DDC BUFF SECTION

UNANNOUNCED

JUSTIFICATION

BY

DISTRIBUTION/AVAILABILITY CODES

DIST. MAIL and/or SPECIAL

[Handwritten signature/initials over the form]

THE **BOEING** COMPANY

COMMERCIAL AIRPLANE DIVISION

RENTON, WASHINGTON

DOCUMENT NO. D6-29356TN

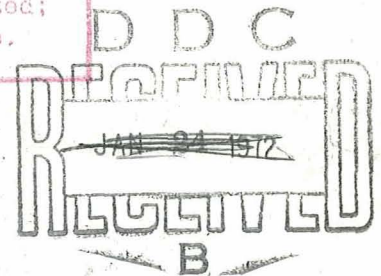
TITLE: OPTIMIZATION OF DUCT LININGS FOR SOUND ATTENUATION

MODEL Research/Contract

ISSUE NO. _____ TO: _____ (DATE) _____

Distribution of this document is unlimited;
it may be released to the general public.

THE WORK DESCRIBED IN THIS REPORT WAS
CARRIED OUT IN PART WITH BOEING CLASS II
RESEARCH FUNDS AND IN PART UNDER NASA
CONTRACT NAS-1-7129.



PREPARED BY Fred W. Fischer 1/12/68
F. W. Fischer

PREPARED BY Anders O. Andersson 1-15-68
A. O. Andersson

SUPERVISED BY J. Brunso & R. Mangiarotti 1-25-68
J. Brunso & R. Mangiarotti

APPROVED BY S. L. S. Jacoby 1-12-68
S. L. S. Jacoby

APPROVED BY J. Large 1/20/68
J. Large

(DATE)

1545 A



LIST OF ACTIVE PAGES

SECTION	PAGE NUMBER	REV SYM	ADDED PAGES						SECTION	PAGE NUMBER	REV SYM	ADDED PAGES						
			PAGE NUMBER	REV SYM	PAGE NUMBER	REV SYM	PAGE NUMBER	REV SYM				PAGE NUMBER	REV SYM	PAGE NUMBER	REV SYM			
	1	A							51									
	2								52	A								
	3	A							53									
	4								54									
	5								55									
	6								56									
	7								57									
	8								58									
	9	A							59									
	10								60									
	11								61									
	12	A							62	A								
	13								63	A								
	14								64	A								
	15								65	A								
	16								66	A								
	17								67	A								
	18								68	A								
	19								69	A								
	20								70	A								
	21								71	A								
	22								72	A								
	23								73	A								
	24								74	A								
	25								75									
	26								76									
	27								77	A								
	28								78									
	29								79									
	30								80									
	31								81									
	32								82									
	33								83									
	34								84									
	35								85									
	36								86									
	37								87									
	38								88									
	39								89									
	40								90									
	41								91									
	42								92									
	43		A						93									
	44		A						94	A								
	45																	
	46																	
	47																	
	48																	
	49	A																
	50																	

AD 1546 B

REV SYM A

REVISIONS

REV SYM	DESCRIPTION	DATE	APPROVAL
A	<p>The work reported in this document is being continued and documented as References 7 and 8 instead of Volumes 2 and 3. The corresponding changes were made in this document. Also, Eqs. (40) and (125) were corrected. In two places ℓ_2 was changed to ℓ_3.</p>	<p>9/24/8 9/25/8 9-26-8</p>	<p><i>[Signature]</i> J. B. <i>[Signature]</i></p>

AD 1048

ABSTRACT

Expressions are derived from which noise attenuation in acoustically lined ducts with and without air flow can be calculated. All possible modes of sound propagation in ducts of various geometries have been considered. Numerical analysis has been carried out to a stage, from which computer programming can be performed. It is shown how the results can be used for the optimum design of inlet and fan duct linings for the reduction of fan noise from jet engines.

KEY WORD LIST

(NOISE-ATTENUATION LINED-DUCTS SOUND-PROPAGATION OPTIMUM-DESIGN
FAN-NOISE SOUND-ATTENUATION DUCT-LINING)

AD 1545 D

TABLE OF CONTENTS

	<u>Page</u>
TITLE PAGE	1
LIST OF ACTIVE PAGES	2
REVISION RECORD	3
ABSTRACT	4
TABLE OF CONTENTS	5
LIST OF ILLUSTRATIONS & TABLES	7
1. SUMMARY	8
1.1 <u>Project Description</u>	8
1.2 <u>Results</u>	9
1.3 <u>Conclusions</u>	9
1.4 <u>Recommendations</u>	11
2. DISCUSSION	12
2.1 <u>Introduction</u>	12
2.2 <u>Mode Attenuation (Rectangular Duct)</u>	18
2.2.1 Solution of the Wave Equation and Boundary Conditions	21
2.2.2 Summary of Analytical Solutions (Table 2)	33
2.2.3 Numerical Solution	34
2.3 <u>Mode Attenuation (Cylindrical and Annular Ducts)</u>	45
2.3.1 Solution of the Wave Equation and Boundary Conditions	45
2.3.2 Summary of Analytical Solutions (Table 3)	55
2.3.3 Numerical Solution	56
2.4 <u>Sound Attenuation in Curved Rectangular Ducts</u>	79
2.4.1 Solution of the Wave Equation	79
2.4.2 Boundary Conditions	79

AD 1546 D

TABLE OF CONTENTS
(continued)

	<u>Page</u>
2.5 <u>Lining Impedance</u>	83
2.5.1 Discrete Element Type	84
2.5.2 Continuous Element Type	85
2.5.3 Composite Lining	86
2.6 <u>Total Attenuation</u>	87
2.7 <u>Subjective Noise and Merit Function</u>	90
2.8 <u>Optimization Program</u>	92
References	94

AD 1546 D



LIST OF ILLUSTRATIONS AND TABLES

<u>Figure</u>		<u>Page</u>
1	Coordinate System	17
2	Graph of $z \tan z$ with $\text{Re} \{ f \}$ as parameter	35
3	Graph of $z \tan z$ with $\text{Im} \{ f \}$ as parameter	37
4	Graph of $-z \cot z$ with $\text{Re} \{ f \}$ as parameter	41
5	Graph of $-z \cot z$ with $\text{Im} \{ f \}$ as parameter	42
6	Graph of $z \frac{J_1(z)}{J_0(z)}$ with $\text{Re} \{ f \}$ as parameter	57
7	Graph of $z \frac{J_1(z)}{J_0(z)}$ with $\text{Im} \{ f \}$ as parameter	58
8	Coordinate System for Curved Duct	80

<u>Table</u>		<u>Page</u>
1	Flow Chart for Acoustic Lining Optimization	10
2	Summary of Analytical Solutions for Rectangular Duct	33
3	Summary of Analytical Solutions for Cylindrical and Annular Ducts	55
4	Starting Points, $\mathcal{N} = 0, 1$	61
5	Starting Points, $\mathcal{N} = 2$ to 8	69
6	Summary of Solution Technique, Cylindrical and Annular Ducts	75



1. SUMMARY

1.1 Project Description

Sound radiated from inlet and fan outlet of turbofan engines gives a major contribution to perceived aircraft noise on the ground, particularly during approach and landing. This sound originates in the fan stages of the engine compressor. By treating inlet and fan duct with sound absorbing linings, the sound can be attenuated in its propagation path. Such linings are built up from a number of pervious layers of different permeability and a number of air spaces of different depths. The particular combination of pervious layers and air spaces determines the magnitude and frequency range of sound attenuation.

In the present duct lining design procedure, experimental results are relied upon. Since the number of lining parameters, that can be varied, is very large, a computer technique was developed by which a pre-selection of multi-layer linings could be performed. These linings, selected to be tested experimentally, are synthesized from pervious layers and air spaces, to give optimum attenuation. The criterion for optimum attenuation of a given engine spectrum is maximum reduction in perceived noise level, i.e., an evaluation of the sound spectrum weighted for the subjective response to the different frequencies of the spectrum.

AD 1545 D



1.2 Results

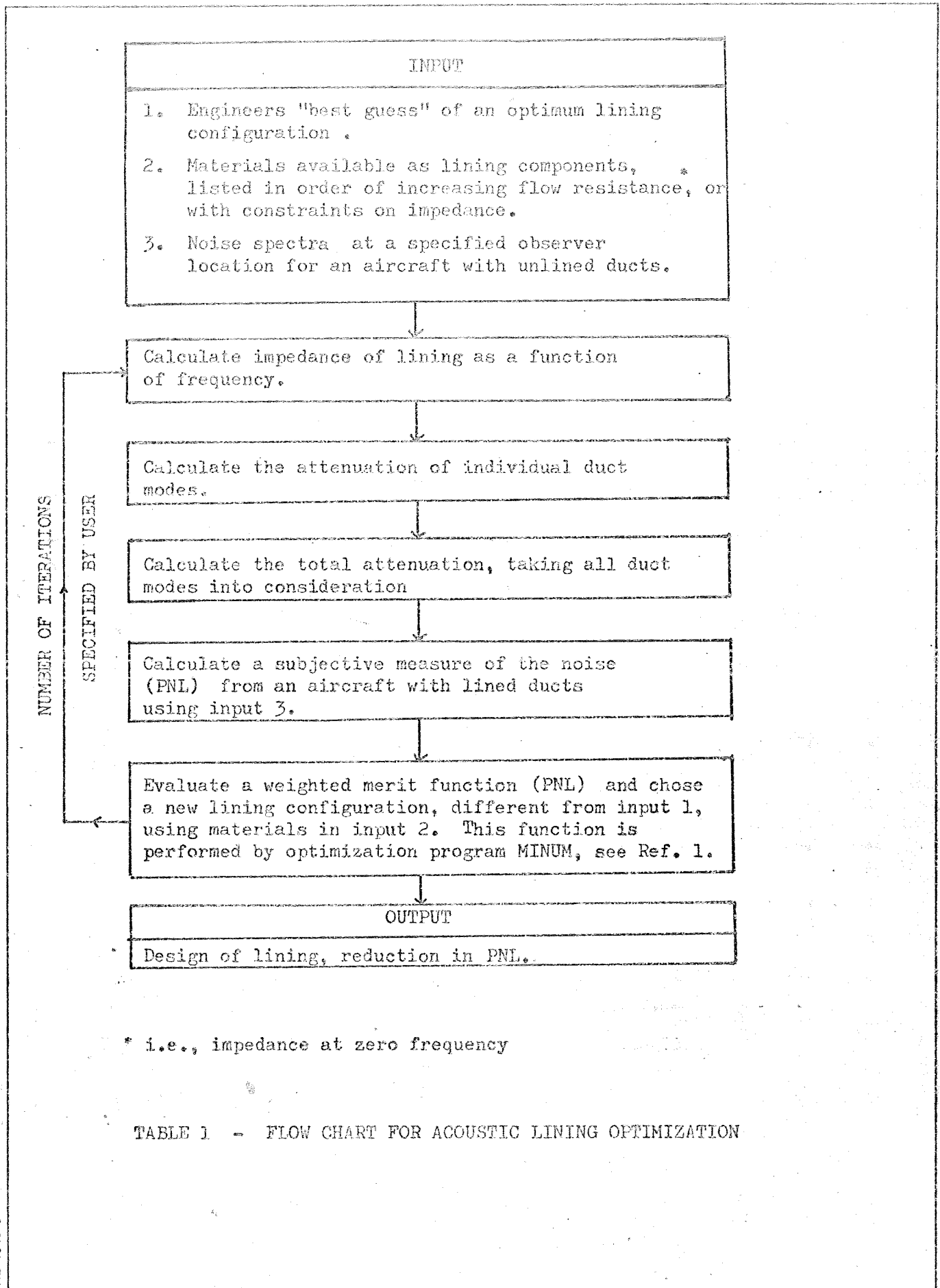
A computer program for the CDC 6600 was developed which provides design parameters of optimum-attenuation multi-layer linings for straight ducts of rectangular, circular, and annular cross-section, and for curved ducts of rectangular cross section. Inputs to the program are the experimentally determined characteristics of a selection of pervious materials, and constraints on thickness of the lining and its individual layers. Optimization of the attenuation can be performed for any number of modes of sound propagation in the duct. A merit function allowing optimization over any frequency range is used.

The flow chart for determining an optimized lining is shown in Table 1. The computer program for straight, rectangular ducts is described in Ref. 7 of this document, and the program for remaining duct shapes in Ref. 8. Typical design problems and their solutions are also presented in References 7 and 8.

1.3 Conclusion

The purpose of computerizing the design of acoustic linings with optimum attenuation has been achieved. Various duct geometries can be handled. The method is limited to "locally reacting" linings, i.e., linings for which the boundary conditions in the duct can be specified completely by the normal incidence impedance of the lining.

AD 1546 D



* i.e., impedance at zero frequency

TABLE 1 - FLOW CHART FOR ACOUSTIC LINING OPTIMIZATION

AD 1545 D



1.4 Recommendations

Further analysis and consequent programming is required on

- * attenuation due to reflection at discontinuities in the impedance of the lining
- * influence of gas velocity in cylindrical and annular ducts.
- * influence of velocity profiles and turbulence.
- * radiation patterns from duct exit taking exit velocity profiles into account.
- * attenuation in lined conical ducts
- * inclusion of a cost function in the merit function for optimization. The cost function would relate weight, volume, and aerodynamic drag of the lining with increase in operating cost of the aircraft.

2. DISCUSSION

2.1 Introduction

In this volume the problem of optimum selection of linings for sound attenuation in ducts of various shapes is analysed. The final result of the analysis is a set of equations, written in a form suitable for direct programming. Corresponding computer programs are presented in References 7 & 8 of this document. The method for optimum selection can be divided in the following steps, each described in detail in the subsequent paragraphs:

- a. Calculation of the attenuation of each mode (type of sound wave propagated) through the duct when the wall impedance (property of the duct wall lining) is specified.
- b. Calculation of the lining impedance from parameters of individual lining elements, such as porous layers and air spaces.
- c. Calculation of total attenuation in the duct taking all modes that can propagate into account simultaneously.
- d. Calculate a value of a merit function, i.e., a function that gives a measure of the efficiency of the lining in attenuating sound.
- e. Optimize lining by choice of lining element parameters which give a minimum value to the merit function.

Return to a. and repeat sequence a specified number of times.

A flow chart showing these steps is also shown in the summary.

The symbols used in this section are (cgs units used throughout):

A, B		Functions of pressure wave amplitude
A_i	}	Defined in Section 2.7
B_i		
C, S	}	Functions of pressure wave amplitude
C_x, S_x		
C_y, S_y		
C, D, G, H		Defined in Section 2.3.1.4
D		Attenuation per unit length of duct (Sec. 2.6)
D_L		Attenuation for duct of length L
D_{mn}		Attenuation per unit length of duct for mode (m,n)
E		Total sound energy in duct
E_{mn}		Energy in mode (m,n)
F, F'	}	Defined where used
G, G'		
K		Defined by Eqs (95) and (124)
IL		Insertion loss
L		Length of duct
L_i		Defined in Section 2.7
M		Mach number
N		Number of evenly-spaced struts, or, for unevenly-spaced struts: $360/\text{angle between 2 adjacent struts}$
N_j	}	Defined in Section 2.7
N_m		
O_j		
PNL		Perceived Noise Level

AD 1546 D

R, Φ, Z, T	Functions of independent variables (used in the solution of the wave equation)
X, Y, Z, T	
V_z	Gas velocity
W	Characteristic impedance
Y	Admittance
Z	Impedance
a, b	Dimensions of duct
c	Speed of sound in air
c_m	Speed of sound in material m
f	Frequency
f, f_1, f_2	Complex constants used in iterations, $= ia l k, ia l_1 k, ia l_2 k$
f_s	Defined by Eqs (94) and (123)
f_r	Ratio of inner to outer radius in annular duct
f_r, f_i	Real and imaginary parts of $f = ia l k$, resp.
j_n	Defined by Eqs (96) and (125)
k	Wave number, $= \frac{2\pi f}{c}$
k_x, k_y, k_z, k_r	Complex wave number in x, y, z, r -directions, resp.
l	Specific admittance
l	Thickness of layer in lining (Sec. 2.5)
l_1, l_2, l_3, l_4	Specific admittances of walls in rectangular duct at $x = 0, x = a, y = 0, y = b$, resp.
m	Order of Bessel function
n	Integer. See Eq. (16)
n	Number of layers in lining (Sec. 2.5)

AD 1545 D



p	Total static pressure, $p = p_0 + p_1$
p_0	Static gas pressure
p_1	Sound pressure
$p_m, t_{m,m+1}, t_{m+1,m}$	Defined in Sec. 2.3.1.4
q_0, r_0, q_0, s_0	See Eq. (62)
r, φ, z	Coordinates
r_m	Mean radius of curved duct
s	Integer, = 1, 2, 3, ... N; used in Tables 3 and 4, mode of Bessel functions of given order and zero value
s_1	Displacement of a fluid particle at a point in the duct lining
s_2	Displacement of a fluid particle in free stream near the duct lining
t	Time
\bar{v}	Total local velocity
v_f	Displacement velocity in free stream
v_n	Gas particle velocity normal to duct walls
v_x	Total velocity in x-direction
v_0	Gas particle velocity due to pressure wave
v_1	Gas velocity
x, y, z	Coordinates
z, z_n, z_{n+1}	Arguments used in iterations, $= ak_x$, ak_y, ak_r
z_r, z_i	Real and imaginary parts of z , resp.
α	Constant of integration in wave equation
α	Attenuation constant, $= \text{Re}$ (Sec. 2.5)

AD 1546 D

α, β	Real and imaginary parts of z , resp. (Sec. 2.3.3)
β	Defined by Eq. (89)
β	Phase constant, = $\text{Im}\{\gamma\}$ (Sec. 2.5)
θ	Strut spacing in radians
γ	Complex propagation constant (Sec. 2.5)
ν	Used in Tables 3 and 4, function of order of Bessel function
ρ, ρ_0, ρ_1	Total local density, static gas density, density due to pressure wave, resp.
ω	Circular frequency, = $2\pi f$

Figure 1 shows the coordinate systems used in the analysis.



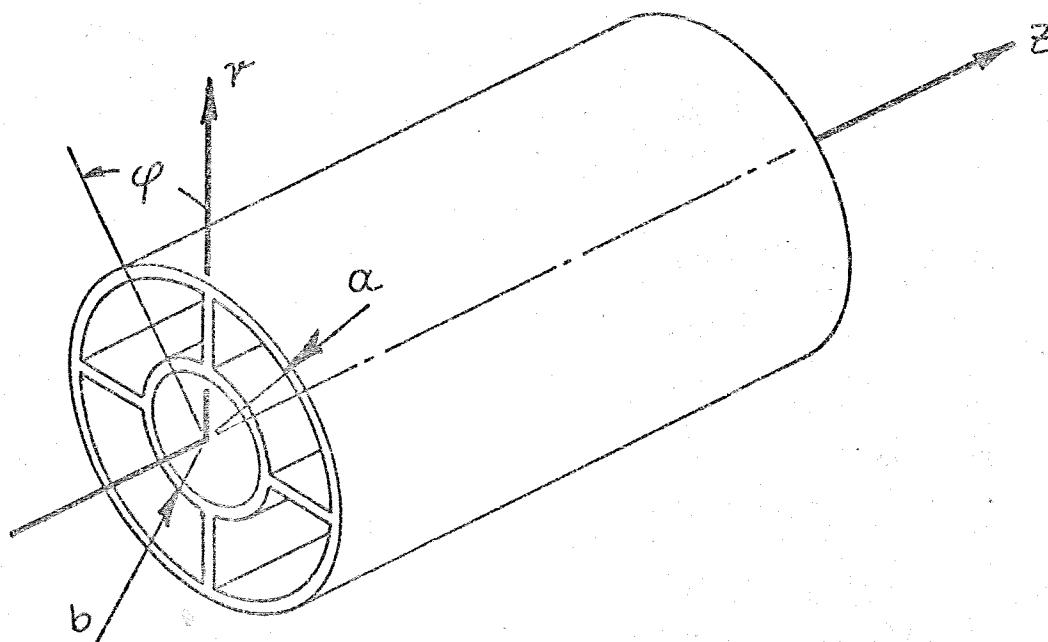
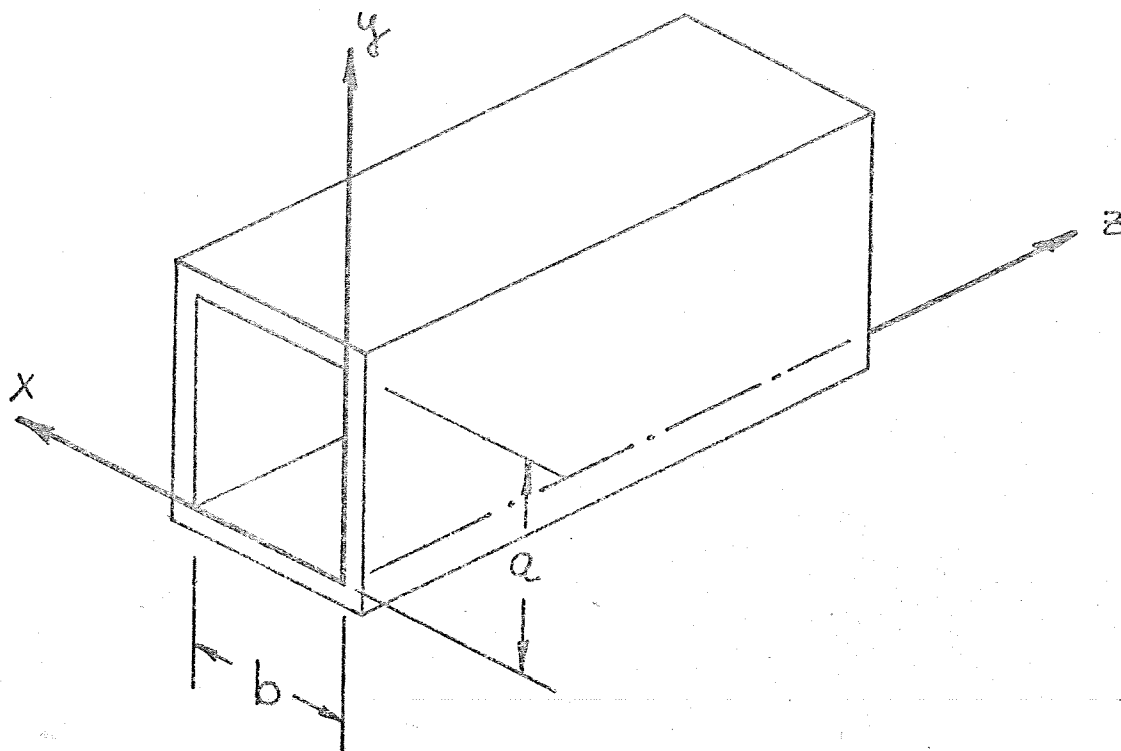


Figure 1
COORDINATE SYSTEM

AD 1545 D

2.2 Mode Attenuation (Rectangular Duct)

The development of the acoustic wave equation is based on Reference 2. Losses due to heat conduction, radiation, and internal friction are assumed small (isentropic case). Also, the gas velocity is assumed small compared to the mean thermal velocity, i.e., speed of sound.

The acoustic wave equation, in the presence of slow unidirectional gas flow, can be derived from the equation of state, the continuity equation, and the equation of motion. Some details of this derivation are shown below.

Total local pressure, density, and velocity can be written as

$$p = p_0 + p_1 = p(\xi) \quad (1)$$

or expanding this equation in a Taylor series with $p_1 = \delta p$

$$p(\xi) = p_0 + \delta p = p_0 + \left. \left(\frac{\partial p}{\partial \xi} \right) \right|_{\xi=\xi_0} \delta \xi + \dots$$

where, for small sound amplitudes,

$$\delta p = \frac{\partial p}{\partial \xi} \delta \xi = c^2 \delta \xi$$

(c being the speed of sound in the medium).

Since p_0 is a constant:

$$dp = dp_1$$

The density and its derivative can be written with $\xi_1 = \delta \xi$ as

$$\xi = \xi_0 + \xi_1 = \xi_0 + \delta \xi \quad (2)$$

$$d\xi = d\xi_1$$



and the velocity and its derivative are

$$\bar{v} = \bar{v}_0 + \bar{v}_1$$

$$d\bar{v} = d\bar{v}_1$$

Equations (1) and (2) may be combined to give

$$p = p_0 + \delta p = p_0 + c^2 \delta \rho$$

$$= c^2 (\rho_0 + \delta \rho) + (p_0 - c^2 \rho_0)$$

$$= c^2 \rho + (\text{constant}) \quad (3)$$

Equation (3) is the equation of state.

The continuity equation is written in vector notation as

$$-\nabla \cdot (\rho \bar{v}) = \frac{d\rho}{dt} \quad (4)$$

Neglecting second order terms, Equation (4) can be rewritten as

$$-\nabla \cdot \bar{v} = \frac{1}{\rho_0} \frac{d\rho}{dt} \quad (5)$$

To obtain Euler's equation of motion, the pressure forces in one direction on an elementary volume are equated to the inertial forces in the same direction:

$$\frac{p(x) - p(x + dx)}{dx} dx dy dz = - \frac{\partial p}{\partial x} dx dy dz$$

$$= \rho_0 \frac{dv_x}{dt} dx dy dz$$

or

$$-\frac{\partial p}{\partial x} = \rho_0 \frac{dv_x}{dt} \quad (6)$$

where it was assumed that second order terms can be ignored for low intensity waves. $\frac{d}{dt}$ again is the total derivative consisting of the local and the convective acceleration terms, resp.,:

$$\frac{d}{dt} = \frac{\partial}{\partial t} + (\bar{v}_0 \cdot \nabla)$$

Equation (6) can be generalized in vector notation:

$$\nabla p + \rho_0 \frac{d\bar{v}}{dt} = 0 \quad (7)$$

Equations (3), (5), and (7) can be combined to eliminate p and \bar{v} .

Substituting Equation (3) into (5) results in

$$\nabla \cdot \bar{v} = -\frac{1}{\rho_0 c^2} \frac{dp}{dt} \quad (8)$$

Taking the divergence of all terms in Equation (7) gives

$$\nabla^2 p + \rho_0 \frac{d}{dt} (\nabla \cdot \bar{v}) = 0$$

and substituting Equation (8) into the last equation:

$$c^2 \nabla^2 p = \left(\frac{d}{dt} \right)^2 p \quad (9)$$

If the gas flow is taken in the z-direction only, Equation (9) becomes

$$c^2 \nabla^2 p = \left(\frac{\partial^2}{\partial t^2} + 2v_z \frac{\partial^2}{\partial t \partial z} + v_z^2 \frac{\partial^2}{\partial z^2} \right) p$$

or

$$c^2 \nabla^2 p = \left(\frac{\partial}{\partial t} + v_z \frac{\partial}{\partial z} \right)^2 p \quad (10)$$

Equation (10) is the acoustic wave equation in the presence of slow, unidirectional gas flow.

2.2.1 Solution of the Wave Equation and Boundary Conditions

Equation (10) can be solved by separation of variables:

$$p = X(x) Y(y) Z(z) T(t) \quad (10a)$$

where

$$X = C_x \cos(k_x x) + S_x \sin(k_x x)$$

$$Y = C_y \cos(k_y y) + S_y \sin(k_y y)$$

$$Z = e^{-ik_z z}$$

$$T = e^{i\omega t}$$

Substituting X, Y, Z and T into Eq. (10) and using

$$k = \frac{\omega}{c}$$

$$M = \frac{v_z}{c}$$

results in

$$k_z = \frac{-kM + [k^2 - (1 - M^2)(k_x^2 + k_y^2)]^{1/2}}{(1 - M^2)} \quad (11)$$

The impedance of a multi-layer lined wall is discussed in Section 2.5. The relationship between k_x or k_y and impedance (or admittance) of the lining can be found from the boundary conditions. If s_1 is defined as the displacement of a point in the lining, and the admittance, L , is defined by $L = v_n/p$:

$$\frac{ds_1}{dt} = Lp \quad (11a)$$

or defining the specific admittance as

$$l = \int_0^c L$$

Eq. (11a) becomes

$$\frac{ds_1}{dt} = \frac{lp}{\int_0^c c}$$

or, integrating,

$$s_1 = \frac{pl}{i\omega \int_0^c c} + \text{constant} \quad (12)$$

If s_2 is defined as the displacement of a fluid particle in the free stream near the duct lining, then

$$s_1 = s_2$$

because, at both sides of the interface of lining and free stream the particles have the same displacement. The displacement velocity in the free stream is

$$v_f = \frac{ds_2}{dt}$$



Substitution into the equation of motion (Eq. (7)) and taking the boundary in the y-z plane gives

$$\frac{d^2 s_2}{dt^2} = -\frac{1}{\rho_0} \frac{\partial p}{\partial x}$$

or with Eq. (12)

$$\frac{\ell}{iec} \left(\frac{d}{dt} \right)^2 p = - \left(\frac{\partial p}{\partial x} \right)_x \text{ at boundary} \quad (12a)$$

or

$$\frac{i\ell}{k} \left[k - k_z M \right]^2 = \pm k_x \frac{\tan(k_x x) - \frac{S_x}{C_x}}{1 + \frac{S_x}{C_x} \tan(k_x x)} \quad (13)$$

where x refers to boundary.

Similarly, if the boundary is taken in the x-z plane, Eq. (13) becomes

$$\frac{i\ell}{k} \left[k - k_z M \right]^2 = \pm k_y \frac{\tan(k_y y) - \frac{S_y}{C_y}}{1 + \frac{S_y}{C_y} \tan(k_y y)} \quad (14)$$

where y refers to boundary. Eqs (13) and (14) are the basic equations along with Eq. (11) used to determine sound attenuation in a rectangular duct. $S_x, S_y, C_x,$ and C_y are eliminated using given boundary conditions.

ℓ, k, M and y are known. When M is equal to zero, k_x is found from Eq. (13), k_y from Eq. (14), and k_z from Eq. (11). When M is not equal to zero, only a few cases of wall linings can be solved without difficulties. The complex number k_z will be used to find the sound attenuation in the ducts.

The sign of the term on the right sides of Eqs (13) and (14) is determined by the direction of the pressure gradient relative to the coordinate system. At $x = 0$ and also at $y = 0$ the minus sign applies; at the respectively opposite walls the plus sign applies.

The following ways to line a rectangular duct are available. The case for zero Mach number is handled separately in Secs 2.2.1.1 to 2.2.1.4. Secs 2.2.1.5 and on deal with solutions of the wave equation when the Mach number is greater than zero but $\ll 1$.

Cases when Mach number is zero:

2.2.1.1 One wall lined only.

$$\begin{array}{l} \text{At } x = 0 \quad \ell = \ell_1 \\ \quad x = a \\ \quad y = 0 \\ \quad y = b \\ \quad M = 0 \end{array} \left. \vphantom{\begin{array}{l} x = a \\ y = 0 \\ y = b \end{array}} \right\} \ell = 0$$

Equation (13) becomes

$$i \ell_1 k = + k_x \frac{S_x}{C_x}$$

and also

$$0 = k_x \frac{\tan(ak_x) - \frac{S_x}{C_x}}{1 + \frac{S_x}{C_x} \tan(ak_x)}$$

AD 1546 D



Eliminating $\frac{S_x}{C_x}$ from the last two equations results in

$$ia \ell_1 k = (ak_x) \tan (ak_x) \quad (15)$$

Eq. (14) becomes

$$0 = k_y \frac{S_y}{C_y}$$

and also

$$0 = k_y \frac{\tan (bk_y) - \frac{S_y}{C_y}}{1 + \frac{S_y}{C_y} \tan (bk_y)}$$

or

$$\tan (bk_y) = 0$$

Therefore

$$k_y = \frac{n\pi}{b} \quad (16)$$

$$n = 0, 1, 2, 3, \dots$$

Equation (15) may be solved numerically for k_x for all modes of interest. Together with k_y , one may find k_z using Eq. (11). This equation may be rewritten for $M = 0$:

$$k_z = \sqrt{k^2 - k_x^2 - k_y^2} \quad (17)$$

2.2.1.2 Adjacent Walls Lined.

When two adjacent walls are lined, Eq. (15) may be used to find k_x for one wall, and a procedure similar to that shown in Section 2.2.1.1 can be applied to find k_y for the adjacent wall. Assume that at $y = 0$ the wall lining has an admittance $l = l_2$, and at $y = b$ the wall is rigid ($l = 0$). Equation (14) may then be written (with $M = 0$):

$$i l_2 k = k_y \frac{S}{C_y}$$

and

$$0 = k_y \frac{\tan(bk_y) - \frac{S}{C_y}}{1 + \frac{S}{C_y} \tan(bk_y)}$$

Again, eliminating $\frac{S}{C_y}$, these equations can be combined to

$$i b l_2 k = (b k_y) \tan(b k_y) \quad (18)$$

Equations (15) and (18) may be solved numerically for k_x and k_y , respectively. k_z may again be obtained by substituting the values into Eq. (17).

2.2.1.3 Two Opposite Walls Lined with linings of same admittance.

$$\begin{aligned} \text{at } & \left. \begin{aligned} x &= 0 \\ x &= a \end{aligned} \right\} l = l_1 \\ & \left. \begin{aligned} y &= 0 \\ y &= a \end{aligned} \right\} l = 0 \\ & M = 0 \end{aligned}$$

Substitution of these boundary conditions into Equation (13) yields

$$i\ell_1 k = k_x \frac{S_x}{C_x}$$

and

$$i\ell_1 k = k_x \frac{\tan(ak_x) - \frac{S_x}{C_x}}{1 + \frac{S_x}{C_x} \tan(ak_x)}$$

Eliminating $\frac{S_x}{C_x}$:

$$\left[\frac{(i\ell_1 k)^2}{k_x} - k_x \right] \tan(ak_x) + 2i\ell_1 k = 0 \quad (19)$$

Equation (19) may be simplified, i.e., the coordinate system may be shifted, so that it takes a form similar to that of Equation (15):

Substitute

$$\tan(ak_x) = \frac{2 \tan\left(\frac{ak_x}{2}\right)}{1 - \tan^2\left(\frac{ak_x}{2}\right)}$$

into Eq. (19). After some simple arithmetic, two equations (Eqs (20) and (21)) are obtained, giving k_x for alternate modes.

$$\frac{ia\ell_1 k}{2} = \frac{ak_x}{2} \tan\left(\frac{ak_x}{2}\right) \quad (20)$$

$$\frac{ia\ell_1 k}{2} = -\frac{ak_x}{2} \cot\left(\frac{ak_x}{2}\right) \quad (21)$$

Equivalently, for the other two walls,

$$\text{when at } \left. \begin{array}{l} y = 0 \\ y = b \end{array} \right\} l = l_2$$

one has

$$\frac{ib l_2 k}{2} = \frac{bk}{2} \tan \left(\frac{bk}{2} \right) \quad (22)$$

$$\frac{ib l_2 k}{2} = - \frac{bk}{2} \cot \left(\frac{bk}{2} \right) \quad (23)$$

2.2.1.4 Two Opposite Walls Lined with Linings of different admittances.

$$\begin{array}{l} \text{at } x = 0 : \quad l = l_1 \\ \quad \quad \quad x = a : \quad l = l_3 \\ \quad \quad \quad M = 0 \end{array}$$

Substitution of these boundary conditions into Eq. (13) yields

$$i l_1 k = k_x \frac{S_x}{C_x}$$

and

$$i l_3 k = k_x \frac{\tan(ak_x) - \frac{S_x}{C_x}}{1 + \frac{S_x}{C_x} \tan(ak_x)}$$

eliminating $\frac{S_x}{C_x}$:

$$\left[\frac{k^2 l_1 l_3}{k_x} + k_x \right] \tan(ak_x) - ik(l_1 + l_3) = 0 \quad (24)$$

If, in addition, at

$$y = 0, \quad l = l_2$$

$$y = b, \quad l = l_4$$

an equation similar to Eq. (24) is obtained

$$\left[\frac{k^2 l_2 l_4}{k_y} + k_y \right] \tan(bk_y) - ik(l_2 + l_4) = 0 \quad (25)$$

No further significant simplification of Eqs (24) and (25) is possible.

Cases When Mach Number is not Zero

2.2.1.5 One Wall Lined Only

$$\text{at } x = 0, \quad l = l_1$$

$$x = a, \quad l = 0$$

Using the same procedure as in Section 2.2.1.1, Eq. (15) now becomes (starting from Eq. (13))

$$\frac{i l_1}{k} [k - k_z M]^2 = k_x \tan(ak_x)$$

or using Eq. (11) to eliminate k_z

$$\frac{i l_1}{k(1-M^2)^2} \left\{ k - M \left[k^2 - (1-M^2)(k_x^2 + k_y^2) \right]^{1/2} \right\}^2 = k_x \tan(ak_x) \quad (26)$$



where, from Eq. (16),

$$k_y = \frac{n\pi}{b}$$

$$n = 0, 1, 2, 3, \dots$$

2.2.1.6 Two adjacent walls lined.

$$\text{at } x = 0, \quad l = l_1$$

$$x = a, \quad l = 0$$

$$y = 0, \quad l = l_2$$

$$y = b, \quad l = 0$$

In this case, Eq. (26) applies; but instead of Eq. (16), an equation similar to Eq. (26) applies:

$$\frac{i l_2}{k(1-M^2)^2} \left\{ k - M \left[k^2 - (1-M^2)(k_x^2 + k_y^2) \right]^{1/2} \right\}^2 = k_y \tan(bk_y) \quad (27)$$

Also, if preferred, the respective sides of Eqs (26) and (27) may be divided by each other, resulting in a new equation which will take the place of Eq. (27) and may be easier to program:

$$\frac{k_x}{l_1} \tan(ak_x) = \frac{k_y}{l_2} \tan(bk_y) \quad (28)$$

Either Eqs (26) and (27) or Eqs (26) and (28) must be solved for

k_x and k_y .



2.2.1.7 Two opposite walls lined with linings of same admittance.

$$\left. \begin{array}{l} x = 0 \\ x = a \end{array} \right\} \ell = \ell_1$$

$$\left. \begin{array}{l} y = 0 \\ y = b \end{array} \right\} \ell = 0$$

Working from Eq. (13) and using the procedure outlined in Section 2.2.1.3, Eqs (29) and (30) may be obtained.

$$\tan \left(\frac{ak_x}{2} \right) = \frac{i\ell_1}{k_x k} (k - k_z M)^2 \quad (29)$$

$$\cot \left(\frac{ak_x}{2} \right) = - \frac{i\ell_1}{k_x k} (k - k_z M)^2 \quad (30)$$

Before solving these equations, k_z from Eq. (11) must be substituted.

If only two walls are lined, Eq. (16) is used to find k_y .

When the other two walls are also lined (at $y = 0$ and at $y = b$;

$\ell = \ell_2$), the following equations may be written directly parallel to Eqs (29) and (30):

$$\tan \left(\frac{bk_y}{2} \right) = \frac{i\ell_2}{k_y k} (k - k_z M)^2 \quad (31)$$

$$\cot \left(\frac{bk_y}{2} \right) = - \frac{i\ell_2}{k_y k} (k - k_z M)^2 \quad (32)$$

2.2.1.8 Two opposite walls lined with linings of different admittances.

$$\text{at } x = 0, \quad \ell = \ell_1$$

$$x = a, \quad \ell = \ell_3$$



As before, starting from Eq. (13) and the above boundary conditions, Eq. (33) can be developed.

$$\left\{ \frac{l_1 l_3}{k^2 k_x} (k - k_z M)^4 + k_x \right\} \tan(ak_x) = \frac{i}{k} (k - k_z M)^2 (l_1 + l_3) \quad (33)$$

For the other two walls this is, equivalently with $l = l_2$ at $y = 0$ and $l = l_4$ at $y = b$,

$$\left\{ \frac{l_2 l_4}{k^2 k_y} (k - k_z M)^4 + k_y \right\} \tan(bk_y) = \frac{i}{k} (k - k_z M)^2 (l_2 + l_4) \quad (34)$$

2.2.2 Summary of Analytical Solutions for Rectangular Duct

TABLE 2

One Wall Only	2 adjacent Walls	2 Opposite Walls (Same Lining)	3 Walls (Oppos. With Same Lining)	4 Walls (Opp. Walls With Same Lining)	2 Opposite Walls (With Different Lining)	3 Walls (Opp. Walls With Different Lining)	4 Walls (Opp. Walls With Different Lining)
---------------	------------------	--------------------------------	-----------------------------------	---------------------------------------	--	--	--

15	15	20	20	20	24	24	24
16	18	21	21	21	16	18	25
17	17	16	18	22	17	17	17
		17	17	23			
				17			

M=0

26	26	26	29	29	29	33	33
16	27	28	30	30	30	16	18
11	11	11	16	27	31	11	11
			11	11	32		
					11		

M ≥ 0

Numbers refer to equations in report which are required to find k_z for a given lining geometry.

2.2.3 Numerical Solution

The acoustic parameters for all cases of lining geometry (shown in Section 2.2.2) can be found by numerical methods. The given parameters in the equations are k (a linear function of sound frequency), ℓ (the admittance of multi-layer lining), a and b (the dimensions of the duct). The problem is to solve the equations for k_z . In this section, only the solution of the equations for k_x and k_y is discussed. k_z may be found without complications from k_x and k_y .

Newton's tangent method was chosen to find solutions for an unlimited number of modes. In this report, only cases for $M = 0$ are covered. Some of the simpler cases with $M > 0$ may be solved by first finding a solution with $M = 0$ and then using iteration methods to find the final solution.

The major problem encountered when using Newton's method is to find suitable starting points. To facilitate this, a plot of Eq. (15) is included which shows an approximately cyclic behavior along the $\text{Re} \{ ak_x \}$ axis. On the graph (Figure 2), ak_x is denoted by z and $ia \ell_1 k$ by f . Both z and f are complex. The mode is determined by the relative magnitude of $\text{Re} \{ z \}$. Therefore, the fundamental (zero) mode is the first solution of Eq. (15) found as one moves up along the vertical axis. Two distinct regions are apparent in the graph: one in which $\text{Re} \{ f \}$ is negative and one in which $\text{Re} \{ f \}$ is positive. The positive regions are well-defined pockets near

Re { z }

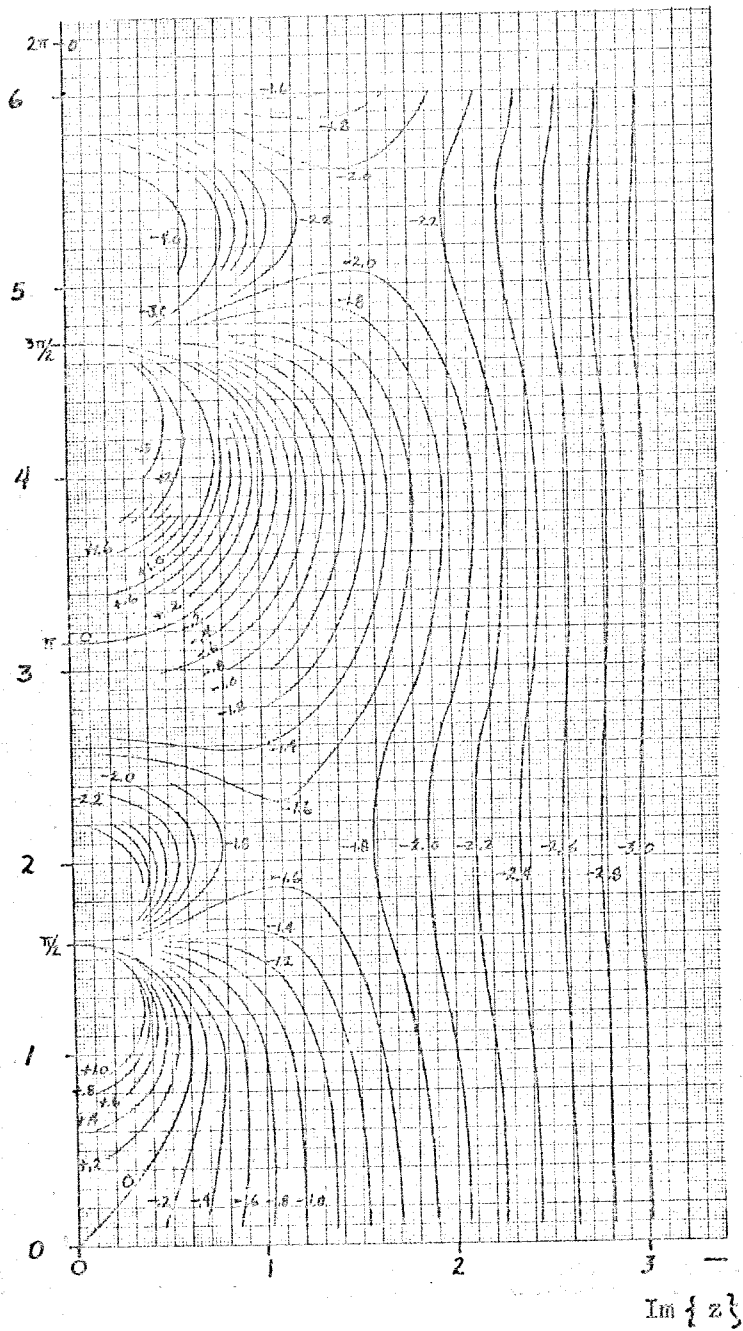


Fig. 2

Graph of $z \tan z$ with $\text{Re} \{ f \}$ as parameter

AD 1545 D



$\text{Im} \{ z \} = 0$. Each of these pockets corresponds to a mode. The negative region is connected for all modes and extends over all values of $\text{Im} \{ z \}$. While Figure 2 was drawn up for $\text{Re} \{ f \}$ as the parameter, Figure 3 was drawn up for $\text{Im} \{ f \}$ as the parameter. The two sets of curves are orthogonal. Figure 2 shows only the first quadrant. The third quadrant is the same as the first turned about the origin through 180° ($f = z \tan z = -z \tan(-z)$). The second and fourth quadrants are of no interest in acoustics.

The iteration equation for the tangent method for solving Eq. (15) for ak_x is

$$z_{n+1} = z_n - \frac{F}{F'} \quad (35)$$

where

$$\begin{aligned} F &= (ak_x) \tan(ak_x) - ia \ell_1 k \\ &= z_n \tan(z_n) - f \end{aligned}$$

and F' is the derivative of F with respect to z evaluated at z_n . Eq. (35) may also be written as

$$z_{n+1} = \frac{2z_n^2 + f(1 + \cos(2z_n))}{2z_n + \sin(2z_n)} \quad (36)$$

When $\text{Re} \{ f \}$ is positive the starting point for all modes is chosen near $\text{Re} \{ z \} = +\infty$; i.e., for the fundamental mode, $\text{Re} \{ z \}$ is $\frac{\pi}{2} - .05$ and $\text{Im} \{ z \}$ is $.02$. For the first mode, $\text{Re} \{ z \}$ is increased by π , while $\text{Im} \{ z \}$ is unchanged. The starting points for all succeeding modes are obtained by increasing the preceding values of $\text{Re} \{ z \}$ by π .

Re { z }

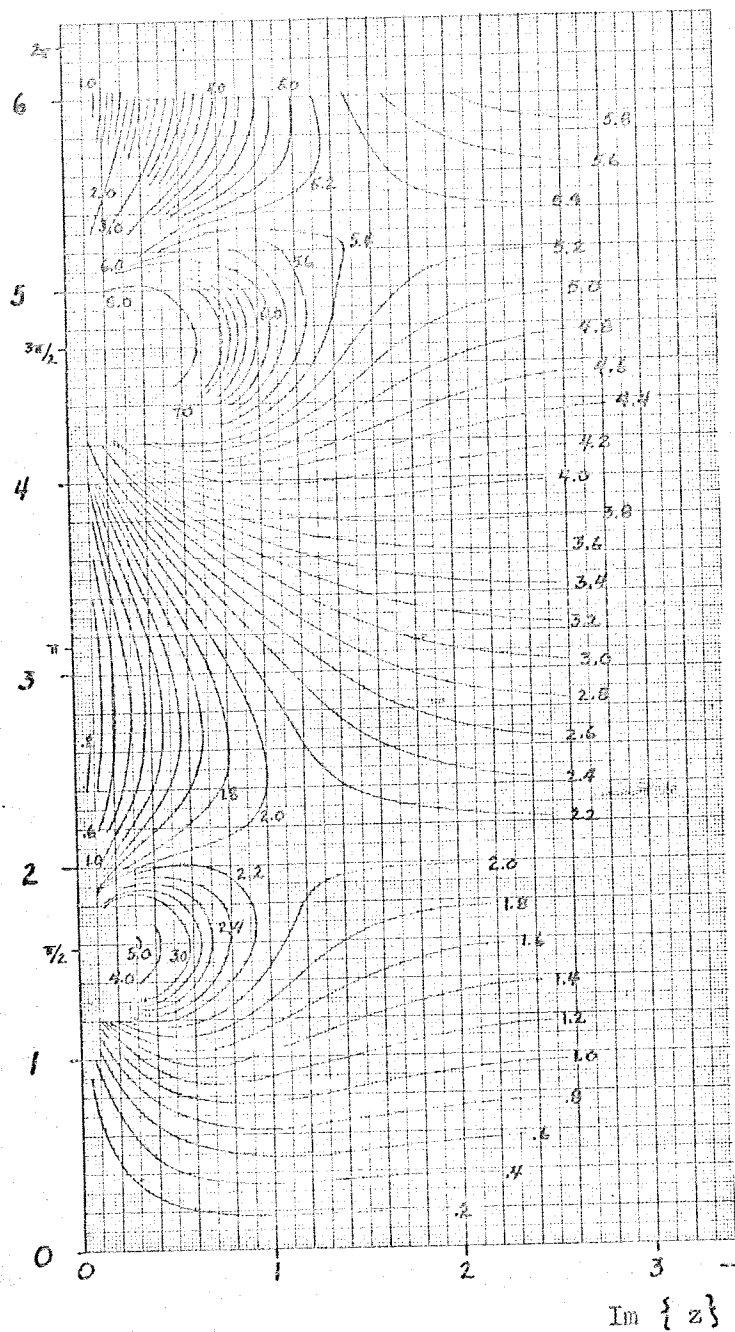


Fig. 3

Graph of $z \tan z$ with $\text{Im} \{ f \}$ as parameter

AD 1546 D



When $\text{Re } \{ f \}$ is negative, the saddle point (for the fundamental mode near $\text{Re } \{ f \} \approx -1.7$) complicates the solution of Eq. (15) for k_x . The Newton method is not applicable at such points. Therefore, a scheme of starting points must be chosen such that for at least one of them, k_x for a given mode is on the same side of the saddle point. This requires that the number of starting points for a given number of modes (from the fundamental up) exceeds the number of modes. For the values of f of interest in acoustic linings it was found that the following starting points gave complete solutions of Eq. (15) for negative values of $\text{Re } \{ f \}$:

$\text{Re } \{ f \}$ near ∞

($\text{Re } \{ z \}$ is $\frac{n\pi}{2} + .05$, with $n = 1, 2, 3, \dots$;

and $\text{Im } \{ z \}$ is .05)

$\text{Re } \{ f \}$ near zero

($\text{Re } \{ z \}$ is $n\pi - .05$, with $n = 1, 2, 3, \dots$;

and $\text{Im } \{ z \}$ again is .05)

However, in some extreme cases, the fundamental mode was not found with these starting points. Therefore, another scheme was devised, taking advantage of the behavior of Eq. (15) at large values of $\text{Im } \{ z \}$. For large values of $\text{Im } \{ z \}$, Eq. (15) can be simplified to

$$f = z \tan z$$

$$= (z_r + iz_i) \frac{\sin(2z_r) + i \sinh(2z_i)}{\cos(2z_r) + \cosh(2z_i)}$$

$$\begin{aligned}
(f_r + if_i) &\approx (z_r + iz_i)i \\
\operatorname{Re} \{ z \} &= \operatorname{Im} \{ f \} \\
\operatorname{Im} \{ z \} &= -\operatorname{Re} \{ f \}
\end{aligned}
\tag{37}$$

Eq. (37) is also used as a starting point when $\operatorname{Re} \{ f \} < 0$ to find the fundamental mode.

To summarize, for $\operatorname{Re} \{ f \} \geq 0$ the number of modes is equal to the number of starting points; i.e., Newton's method is applicable in the entire region (for each mode). The values of k_x are found in the order of increasing modes as n is increased from 1 to the value of the number of modes desired.

For $\operatorname{Re} \{ f \} < 0$ the values of k_x will not necessarily be in the order of increasing modes; also, some values of k_x may appear many times over as n is increased. Therefore, in computer programming, a subprogram is required to eliminate duplicate values of k_x and to order the remaining values of k_x according to the increasing magnitude of $\operatorname{Re} \{ k_x \}$.

Equation (18) has the same form as Eq. (15), and is solved for k_y in the same fashion as Eq. (15) is solved for k_x .

In general, the above scheme can also be used to solve Eqs (20) and (22). In this case, $z = \frac{ak_y}{2}$ or $\frac{ak_y}{2}$ and $f = \frac{ial_1k}{2}$ or $\frac{ibl_2k}{2}$.

Equations (21) and (23), however, are slightly different. For these, Figures 4 and 5 were drawn up. In general, the pattern is very similar to that shown in Figures 2 and 3. Only the starting points must be changed:

$$\text{For } \operatorname{Re} \{ f \} \geq 0$$

$$\operatorname{Re} \{ z \} \text{ is } n\pi - .05 \quad (n = 1, 2, 3, \dots)$$

$$\operatorname{Im} \{ z \} \text{ is } .02$$

$$\text{For } \operatorname{Re} \{ f \} < 0$$

$$\operatorname{Re} \{ z \} \text{ is } (n - 1/2)\pi - .05 \quad (n = 1, 2, 3, \dots)$$

$$\text{and } \operatorname{Re} \{ z \} \text{ is } n\pi + .05 \quad (n = 1, 2, 3, \dots)$$

$$(\text{in both case } \operatorname{Im} \{ z \} = .05)$$

also, for $\operatorname{Re} \{ f \} < 0$

$$\operatorname{Re} \{ z \} = \operatorname{Im} \{ f \}$$

$$\operatorname{Im} \{ z \} = -\operatorname{Re} \{ f \}$$

The iteration equation for the tangent method for solving Eqs (21) and (23) for $(\frac{ak_x}{2})$ and $(\frac{bk_y}{2})$, respectively, is

$$z_{n+1} = z_n - \frac{G}{G'} \quad (38)$$

where

$$G = z_n \cot z_n + f$$

and G' is the derivative of G with respect to z evaluated at z_n .

$$f = \frac{ia l_1 k}{2}, \text{ respectively, } \frac{ib l_2 k}{2}$$

$$z_n = \frac{ak_x}{2}, \text{ respectively, } \frac{bk_y}{2}$$



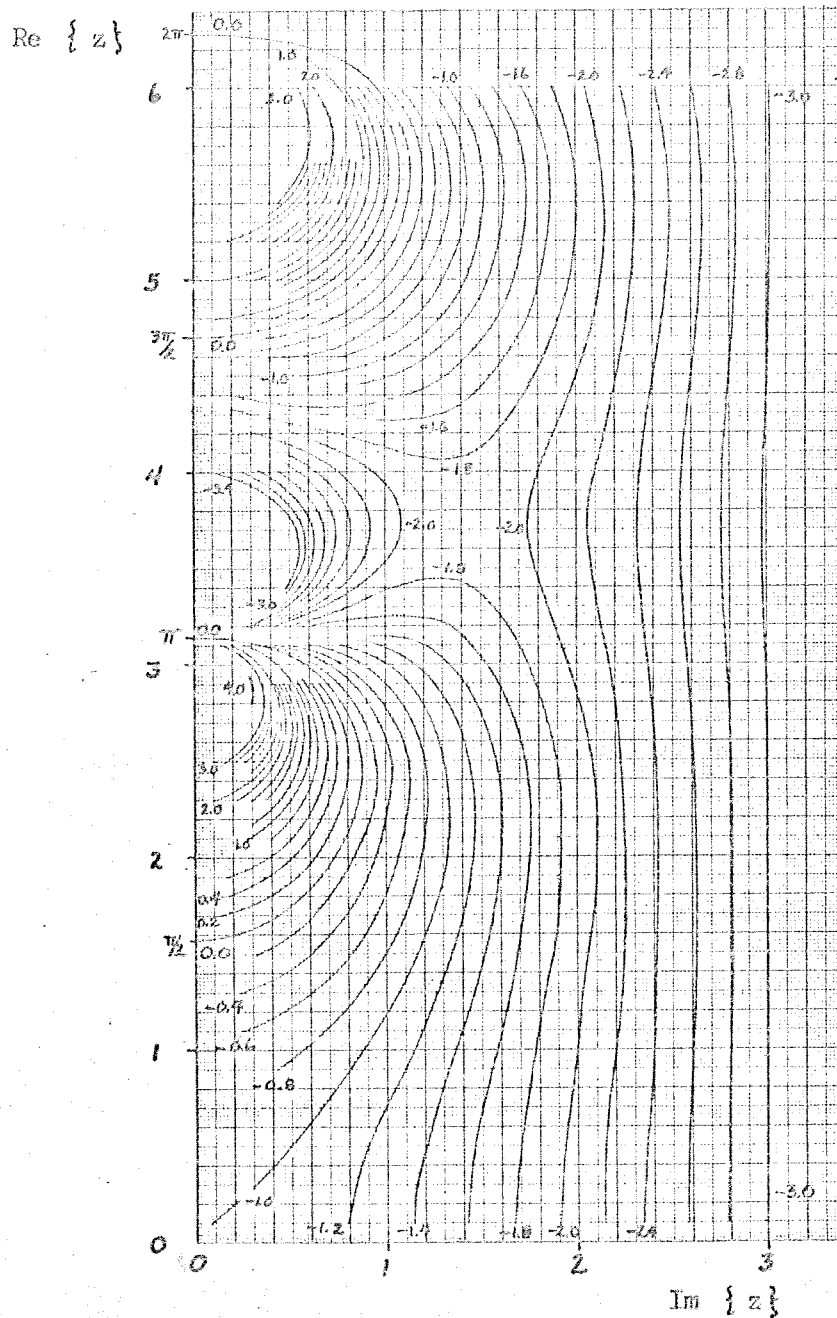


Fig. 4

Graph of $-z \cot z$ with $\text{Re } \{ f \}$ as parameter

AD 1576 D



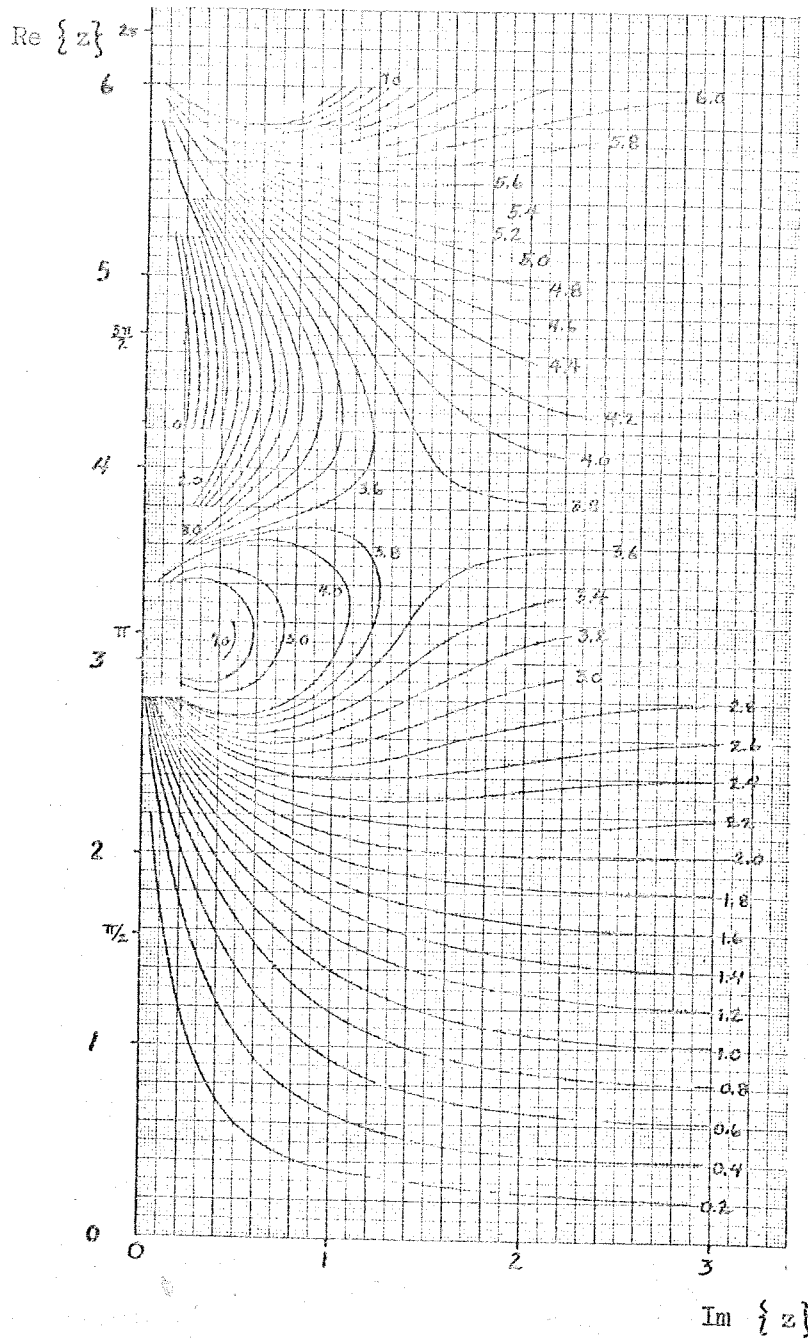


Fig. 5

Graph of $-z \cot z$ with $\text{Im } \{z\}$ as parameter

AD 1545 D

Equation (38) may also be written as

$$z_{n+1} = \frac{2z_n^2 + f(1 - \cos 2z_n)}{2z_n - \sin 2z_n} \quad (39)$$

The solution of Eqs (24) and (25) for k_x and k_y , respectively, is somewhat more difficult. In general, a graph of these equations would look like Figure 2 with the positive zones shifted upward. The starting points for the iterative solution of such equations, therefore depend on the values of the admittances. The relation is very complex. For this reason an approach different from the above was used.

To solve Eqs (24) and (25), l_3 (respectively, l_4) was set equal to zero, which reduced those equations to the form of Eq. (15), respectively, Eq. (18). Below, reference will be made only to Eq. (24), but all remarks also hold for Eq. (25). Equation (15) is solved as described above, and k_x so found is now the starting point for the iterative solution of Eq. (24).

For some values of l_1 this will not give all the modes. Therefore, the process is repeated, this time setting l_1 equal to zero. In some cases (especially where $\text{Im} \{f_1\}$ and $\text{Im} \{f_2\}$ * are larger than 2, and where $\text{Re} \{f_1\}$ or $\text{Re} \{f_2\}$ or both are positive), the fundamental, first, and second modes were missing. Here, the solution started from the problem of a duct with the same lining on opposite walls. That lining (l_1 or l_3) was chosen for this procedure for

* See Equation (41)

which $\text{Re}\{f\}$ was positive. Should further difficulties occur which cause some modes to be omitted, one may also use the other lining. Now, Eq. (24) reduces to Eqs (20) and (21). The solution of the latter equations provided new starting points for each mode of the iterative solution of Eq. (24). The iteration equation for the tangent method for solving Eqs (24) and (25) for ak_x and ak_y , respectively, is

$$z_{n+1} = z_n \frac{z_n (f_1 + f_2) \cos^2 z_n + 2f_1 f_2 \sin z_n \cos z_n - z_n (f_1 f_2 - z_n^2)}{(f_1 f_2 + z_n^2) \sin z_n \cos z_n - z_n (f_1 f_2 - z_n^2)} \quad (40)$$

where

$$\begin{aligned} z_n &= a(k_x)_n, \text{ respectively } b(k_y)_n \\ f_1 &= iakl_1, \text{ respectively } ibkl_2 \\ f_2 &= iakl_3, \text{ respectively } ibkl_4 \end{aligned} \quad (41)$$

2.3 MODE ATTENUATION (CYLINDRICAL AND ANNULAR DUCTS)

The acoustic wave equation was developed in Section 2.2. Losses due to heat conduction, radiation, and internal friction were ignored. The wave equation then is

$$c^2 \nabla^2 p = \left(\frac{d}{dt}\right)^2 p \quad (42)$$

Neglecting gas velocity, Eq. (42) becomes, in cylindrical coordinates,

$$\frac{\partial^2 p}{\partial t^2} = c^2 \left[\frac{1}{r} \frac{\partial}{\partial r} \left(r \frac{\partial p}{\partial r} \right) + \frac{1}{r^2} \frac{\partial^2 p}{\partial \varphi^2} + \frac{\partial^2 p}{\partial z^2} \right] \quad (43)$$

The axisymmetric and asymmetric cases are handled separately even though the axisymmetric case is a special solution of the asymmetric case.

2.3.1 Solution of the Wave Equation and Boundary Conditions

Equation (43) can be solved by separation of variables:

$$p = R(r) \phi(\varphi) Z(z) T(t) \quad (44)$$

Substituting Eq. (44) into Eq. (43) results in

$$\left[\frac{1}{R} \frac{\partial^2 R}{\partial r^2} + \frac{1}{r} \frac{1}{R} \frac{\partial R}{\partial r} + \frac{1}{r^2} \frac{\partial^2 \phi}{\phi \partial \varphi^2} \right] + \left[\frac{1}{Z} \frac{\partial^2 Z}{\partial z^2} \right] = \frac{1}{c^2} \frac{1}{T} \frac{\partial^2 T}{\partial t^2} \quad (45)$$

for the pressure wave along the duct axis one has

$$ZT = e^{i(\omega t - k_z z)} \quad (46)$$

and for the azimuthal pressure wave one has

$$\phi = C \cos(m\varphi) + S \sin(m\varphi) \quad (47)$$

The solution of Eq. (45) for R is then

$$R = AJ_m(k_r r) + BN_m(k_r r) \quad (48)$$

where

$$k_r = (k^2 - k_z^2)^{1/2} \quad (49)$$

The general solution of Eq. (42) is therefore

$$p = [AJ_m(k_r r) + BN_m(k_r r)] \cdot [C \cos(m\varphi) + D \sin(m\varphi)] \cdot e^{i(\omega t - k_z z)} \quad (50)$$

The order and the argument of the Bessel functions J_m and N_m may be complex.

2.3.1.1 Cylindrical Duct with Axisymmetric Pressure Distribution

For this case, Eq. (50) can be simplified to

$$p = AJ_0(k_r r) e^{i(\omega t - k_z z)} \quad (51)$$

since $N_0(k_r r)$ goes to infinity at $r = 0$, and $p = RZT$.

With the assumption that $V_z = 0$, Euler's equation can be written as

(see Section 2.2)

$$\frac{\partial \bar{v}}{\partial t} = -\frac{1}{\rho_0} \nabla p$$

or

$$\left(\frac{v}{n} \right)_{r=a} = -\frac{1}{i\omega\rho_0} \left(\frac{\partial p}{\partial r} \right)_{r=a} \quad (52)$$



From the definition of admittance one has

$$(v_n)_{r=a} = \frac{\ell}{\rho_0 c} (p)_{r=a} \quad (53)$$

Equating the right sides of Eqs (52) and (53) and substituting p from Eq. (51) an equation for k_r is found:

$$ia\ell k = (ak_r) \frac{J_1(ak_r)}{J_0(ak_r)} \quad (54)$$

Equation (54) is similar in form to Eq. (15). The latter can be rewritten as

$$ia\ell k = (ak_x) \frac{\sin(ak_x)}{\cos(ak_x)} \quad (55)$$

The solution of Eq. (54) for k_r follows that of Eq. (55) for k_x .

The attenuation along the duct axis is obtained from k_z which is calculated using Eq. (49)

$$k_z = (k^2 - k_r^2)^{1/2} \quad (56)$$

If the duct has a rigid wall (no lining), then from Eq. (54)

$$J_1(ak_r) = 0 \quad (57)$$

In this case, k_r is real.

For this and all following cases it will be assumed that the lining is the same on all walls. The only exception occurs when struts in annular ducts are lined (Section 2.3.1.5).

2.3.1.2 Annular Duct with Axisymmetric Pressure Distribution

Since there is no requirement for a solution of Eq. (42) at $r = 0$, the Bessel function of the second kind is retained:

$$p = \left[AJ_0(k_r r) + BN_0(k_r r) \right] e^{i(\omega t - k_z z)} \quad (58)$$

If the radius of the outer cylinder is a , and Eqs (52) and (53) are used, then one has

$$ia \ell k = ak_r \frac{AJ_1(ak_r) + BN_1(ak_r)}{AJ_0(ak_r) + BN_0(ak_r)} \quad (59)$$

Equivalently, for the outer surface of the inner cylinder of radius b

$$\begin{aligned} (v_n)_{r=b} &= \frac{1}{i\omega \rho_0} \left(\frac{\partial p}{\partial r} \right)_{r=b} \\ &= \frac{\ell}{c \rho_0} (p)_{r=b} \end{aligned}$$

and then

$$ib \ell k = -bk_r \frac{AJ_1(bk_r) + BN_1(bk_r)}{AJ_0(bk_r) + BN_0(bk_r)} \quad (60)$$

Eliminating A and B from Eqs (59) and (60) gives

$$\frac{fN_0(z) - zN_1(z)}{fJ_0(z) - zJ_1(z)} = \frac{fN_0(f_r z) + zN_1(f_r z)}{fJ_0(f_r z) + zJ_1(f_r z)}$$

or

$$zf(q_0 - r_0) + z^2 s_0 - f^2 p_0 = 0 \quad (61)$$



where

$$\begin{aligned}
 q_o &= J_1(f_r z) N_o(z) - J_o(z) N_1(f_r z) \\
 p_o &= J_o(z) N_o(f_r z) - J_o(f_r z) N_o(z) \\
 r_o &= J_o(f_r z) N_1(z) - J_1(z) N_o(f_r z) \\
 s_o &= J_1(z) N_1(f_r z) - J_1(f_r z) N_1(z) \\
 f &= ia \ell k \\
 f_r &= b/a \\
 z &= ak_r
 \end{aligned}
 \tag{62}$$

If the inner wall is rigid, Eq. (60) reduces to

$$\frac{A}{B} = - \frac{N_1(bk_r)}{J_1(bk_r)}
 \tag{63}$$

Eliminating A and B from Eqs (59) and (63) and using the definitions in Eq. (62) results in a simplification of Eq. (61):

$$f = -z \frac{s_o}{q_o}
 \tag{64}$$

If the outer wall is rigid, Eq. (59) reduces to

$$\frac{A}{B} = - \frac{N_1(ak_r)}{J_1(ak_r)}
 \tag{65}$$

Eliminating A and B from Eqs (60) and (65) results in

$$f = z \frac{s_o}{r_o}
 \tag{66}$$

If the inner and the outer walls are rigid, one has from Eq. (59)

$$AJ_1(ak_r) + BN_1(ak_r) = 0
 \tag{67}$$

AD 1548 D

and from Eq. (59)

$$AJ_1(bk_r) + BN_1(bk_r) = 0 \quad (68)$$

Eliminating A and B results in

$$s_0 = 0 \quad (69)$$

or

$$\frac{J_1(z)}{N_1(z)} = \frac{J_1(f_r z)}{N_1(f_r z)}$$

In this case k_r is real.

2.3.1.3 Cylindrical Duct with Asymmetric Pressure Distribution

The azimuthal term must be retained for this case, and Eq. (51)

is modified to

$$p = AJ_m(k_r r) \cos m(\varphi - \alpha) e^{i(\omega t - k_z z)} \quad (70)$$

where A and α are constants of integration.

With Eqs (52) and (53) one has then

$$(i a \ell k + m) = ak_r \frac{J_{m+1}(ak_r)}{J_m(ak_r)} \quad (71)$$

where $m = 0, 1, 2, 3, \dots$. When $m = 0$, Eq. (71) reverts to Eq. (54).

For a rigid wall, Eq. (71) becomes

$$m = ak_r \frac{J_{m+1}(ak_r)}{J_m(ak_r)} \quad (72)$$

2.3.1.4 Annular Duct with Asymmetric Pressure Distribution

The pressure distribution may be written

$$p = \left[AJ_m(k_r r) + BN_m(k_r r) \right] \cos \left[m(\varphi - \alpha) \right] e^{i(\omega t - k_z z)} \quad (73)$$

where $m = 0, 1, 2, 3, \dots$. Using the same procedure as in 2.3.1.2

one can find the equation for k_r :

$$CD p_m - GH p_{m+1} + CH t_{m, m+1} - DG t_{m+1, m} = 0 \quad (74)$$

where

$$C = iak\ell + m$$

$$D = ibk\ell - m$$

$$G = ak_r = z$$

$$H = bk_r = f_r z$$

$$p_m = J_m(z) N_m(f_r z) - J_m(f_r z) N_m(z)$$

$$t_{m, m+1} = J_m(z) N_{m+1}(f_r z) - J_{m+1}(f_r z) N_m(z)$$

$$t_{m+1, m} = J_{m+1}(z) N_m(f_r z) - J_m(f_r z) N_{m+1}(z)$$

If the inner wall is rigid, Eq. (74) is somewhat simpler:

$$m(C p_m - G t_{m+1, m}) + H(G p_{m+1} - C t_{m, m+1}) = 0 \quad (75)$$

If, in addition, the outer wall is also rigid, Eq. (74) becomes

$$m^2 p_m - m(G t_{m+1, m} + H t_{m, m+1}) + GH p_{m+1} = 0 \quad (76)$$

If only the outer wall is rigid, Eq. (74) becomes

$$m(Dp_m + H t_{m,m+1}) - G(Hp_{m+1} + Dt_{m+1,m}) = 0 \quad (77)$$

2.3.1.5 Annular Duct with Radial Struts

At the strut wall at $\varphi = 0$:

$$(v_n)_{\varphi=0} = \frac{1}{i\omega \rho_0} \left(\frac{1}{r} \frac{\partial p}{\partial \varphi} \right)_{\varphi=0} = (p)_{\varphi=0} \frac{\ell_2}{c \rho_0} \quad (78)$$

Using Eq. (73), Eq. (78) becomes

$$\tan(m\alpha) = \frac{i \ell_2 k_r}{m} \quad (79)$$

If the struts are equally spaced, and assuming negligible thickness, one has at the strut wall at $\varphi = \frac{2\pi}{N}$

$$(v_n)_{\varphi = \frac{2\pi}{N}} = \frac{1}{i\omega \rho_0} \left(\frac{1}{r} \frac{\partial p}{\partial \varphi} \right)_{\varphi = \frac{2\pi}{N}} = (p)_{\varphi = \frac{2\pi}{N}} \frac{\ell_2}{c \rho_0} \quad (80)$$

where $N = 1, 2, 3, \dots$ = number of struts. Substituting for p , Eq. (80) becomes

$$\tan m \left(\frac{2\pi}{N} - \alpha \right) = \frac{i \ell_2 k_r}{m} \quad (81)$$

Eliminating α between Eq. (79) and (81), one has finally

$$\left(\frac{\pi}{N} m \right) \tan \left(\frac{\pi}{N} m \right) = i \ell_2 k \frac{\pi}{N} r \quad (82)$$

The parameter m is, therefore, a function of r . However, the solution of Eq. (43) by separation of variables was based on the

assumption that m (and therefore ϕ) is independent of r . Thus, Eq. (82) may only be used when

$$l_2 r = \text{constant} \quad (83)$$

The problem is now one of manufacturing such a lining.

The parameter m is a complex number, and even though Eq. (74) is applicable, the Bessel functions are now of complex order. If the struts are rigid and not lined, Eq. (82) becomes

$$\tan\left(\frac{\pi}{N} m\right) = 0 \quad (84)$$

or

$$m = N n \quad (85)$$

where $N = 0, 1, 2, 3, \dots$ and $n = 0, 1, 2, 3, \dots$. In this case m is independent of r and a real integer. Eq. (74) applies for finding k_r .

If only the outer cylinder wall is lined, m is determined by Eq. (85) and k_r is determined by Equation (75).

If only the inner wall is lined, m again is found from Eq. (85), and k_r is found from Eq. (77).

If both cylinder walls are lined, m from Eq. (85) is substituted into Eq. (74) to find k_r .

If no walls are lined, m from Eq. (85) is substituted into Eq. (76).

When the struts are not equally spaced, each duct section involving a different spacing must be computed separately. While one strut wall may always be taken at $\varphi = 0$, the other is located at $\varphi = \Theta$, where Θ is the corresponding strut spacing in radians. Eq. (84) now becomes

$$\tan\left(\frac{\Theta}{2} m\right) = 0 \quad (85a)$$

or

$$m = \frac{2\pi}{\Theta} n \quad (85b)$$

In this case m is a real number, but not necessarily an integer.

2.3.1.6 Annular Duct with Asymmetric Pressure Distribution, Gas Velocity Other Than Zero

When the gas velocity is not zero, Eq. (56) becomes

$$k_z = \frac{-kM + [k^2 - k_r^2(1 - M^2)]^{1/2}}{1 - M^2} \quad (85c)$$

For an annular duct with asymmetric pressure distribution, Eq. (74) still holds, except C and D are now defined by

$$C = \frac{i\ell}{ak} \left[\frac{ak - M [a^2 k^2 - G^2(1 - M^2)]^{1/2}}{1 - M^2} \right]^2 + m \quad (85d)$$

$$D = \frac{i\ell}{bk} \left[\frac{bk - M [b^2 k^2 - H^2(1 - M^2)]^{1/2}}{1 - M^2} \right]^2 - m \quad (85e)$$

Equations (75), (76), and (77) may also be solved with C and D defined by Eqs (85d) and (85e).

2.3.2 Summary of Analytical Solutions for Cylindrical and Annular Ducts

TABLE 3

REFERENCES TO EQUATIONS WHICH ARE REQUIRED TO OBTAIN

VARIOUS LINING GEOMETRIES (NUMBERS REFER TO EQUATIONS IN TEXT)

	CYLINDRICAL		ANNULAR		ANNULAR WITH STRUTS
	AXISYMM. ASYMM.	71	AXISYMM. ASYMM.	74	
ALL WALLS LINED	54	71	61	74	82 83 74 56
INTERNAL LINING ON OUTER CYL. ONLY		56	56	56	75 85 or 85b 56
EXTERNAL LINING ON INNER CYL. ONLY			64	75	
			56	56	
			66	77	77 85 or 85b 56
			56	56	
CYLINDRICAL SURFACES LINED ONLY					74 85 or 85b 56
NO LINING	57	72	69	76	76 85 or 85b 56
	56	56	56	56	

2.3.3 Numerical Solution

The acoustic parameters for all cases of lining geometry (shown in Table 3) can be found by numerical methods.

The given parameters in the equations of the previous sections are k (a linear function of sound frequency), \mathcal{L} (the admittance of multi-layer lining), a and b (the radii of the cylindrical and annular ducts). The problem is to solve the equations (Table 3) for k_z . In this section, only the solution for k_r (and, where appropriate, m) is discussed. k_z is found from Eq. (56).

Just as for the rectangular duct, Newton's tangent method was chosen to find solutions for an unlimited number of modes. To facilitate finding starting points for the iterative solution of Eq. (54), Figures 6 and 7 were drawn. On the graphs, ak_r is denoted by z and $ia\mathcal{L}k$ by f . Both z and f are complex. The mode is determined by the relative magnitude of $\text{Re} \{ z \}$. Therefore, the fundamental (zero) mode is the first solution of Eq. (54) found as one moves up along the vertical axis. Two distinct regions are apparent in the graph: one in which $\text{Re} \{ f \}$ is negative and one in which it is positive. The positive regions are well-defined pockets near $\text{Im} \{ z \} = 0$. Each of these pockets corresponds to a mode. The negative region is connected for all modes and extends over all values of $\text{Im} \{ z \}$. Figure 6 was drawn for $\text{Re} \{ f \}$ as

Re { z }

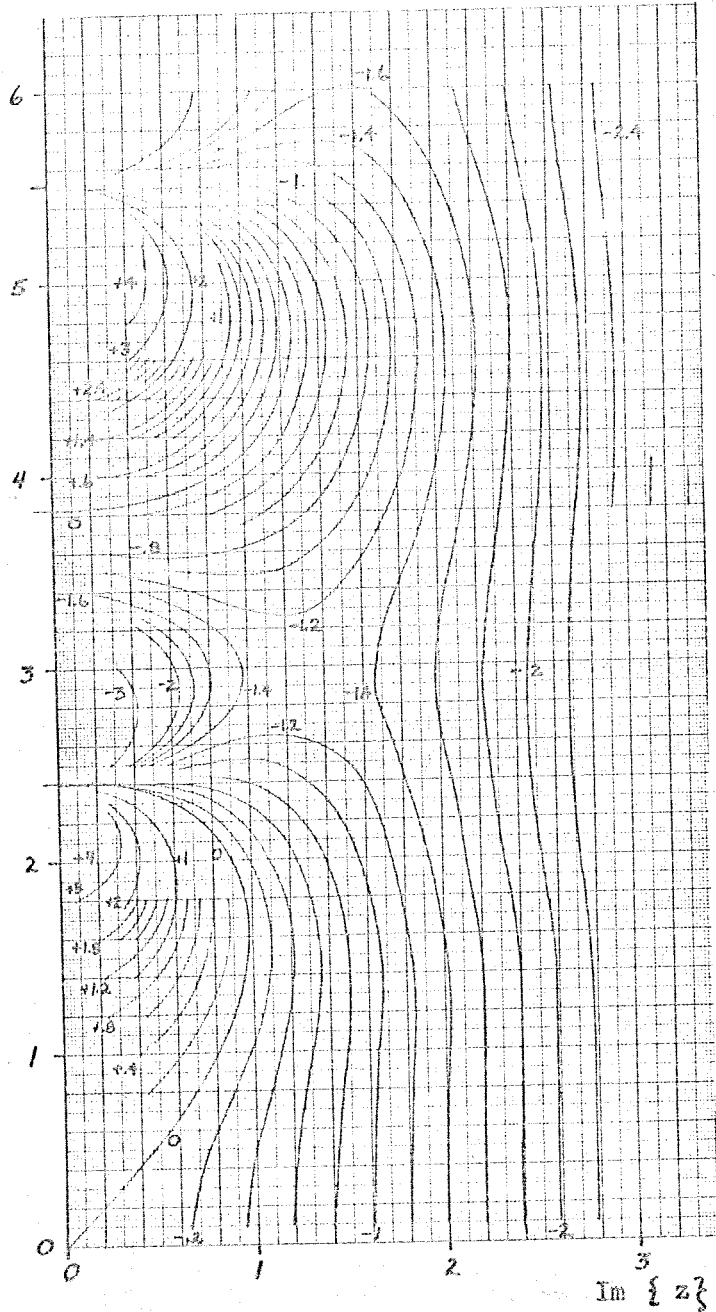


Fig. 6

Graph of $zJ_1(z)/J_0(z)$ with $\text{Re } \{ f \}$ as Parameter

AD 1546 D



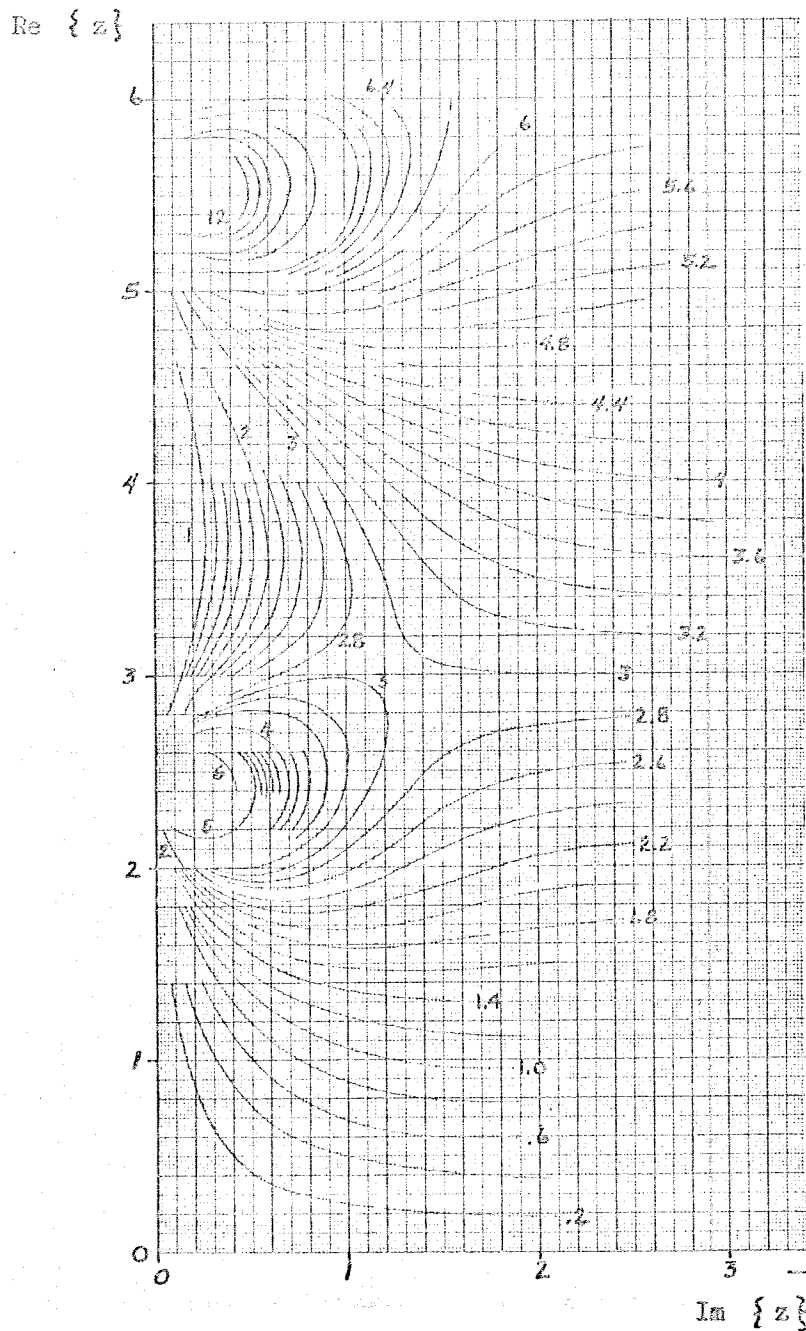


Fig. 7

Graph of $zJ_1(z)/J_0(z)$ with $\text{Im} \{ f \}$ as Parameter

AD 1545 D



as the parameter, and Figure 7 for $\text{Im} \{ f \}$ as the parameter. The two sets of curves are orthogonal. Figure 6 shows only the first quadrant. The third quadrant is the same as the first turned about the origin through 180° . The second and fourth quadrants are of no interest in acoustics.

The iteration equation for the tangent method for solving Eq. (54) for ak_r is

$$z_{n+1} = z_n - \frac{F}{F'} \quad (86)$$

where

$$\begin{aligned} F &= ia \ell k - (ak_r) \frac{J_1(ak_r)}{J_0(ak_r)} \\ &= f - z_n \frac{J_1(z_n)}{J_0(z_n)} \end{aligned}$$

and F' is the derivative of F with respect to z evaluated at z_n .

Equation (86) may also be written as

$$z_{n+1} = z_n + \frac{f - z_n \frac{J_1(z_n)}{J_0(z_n)}}{z_n \left[1 + \left(\frac{J_1(z_n)}{J_0(z_n)} \right)^2 \right]} \quad (87)$$

When $\text{Re} \{ f \}$ is positive, the starting point for all modes is chosen near $\text{Re} \{ f \} = +\infty$. The equations for the starting points were taken from Reference 3 and adjusted for this application. It should be noted that the points of $\text{Re} \{ f \} = 0$ do not occur at regular intervals along the ordinate of Figure 6. The equation for

the starting points for all modes is

$$\operatorname{Re} \{ z \} = \beta + \frac{1}{8\beta} - \frac{4(31)}{3(8\beta)^3} + \frac{32(3779)}{15(8\beta)^5} - \dots - .01 \quad (88)$$

where

$$\beta = (s - 1/4) \pi \quad (89)$$

and $s = 1, 2, 3, \dots, N$.

N is the number of modes required.

The number of terms in Eq. (88) to be retained is critical only with respect to any possibility of crossing the $\operatorname{Re} \{ f \} = 0$ line. Retaining the first three terms and the "stand-off factor" $(-.01)$, Eq. (88) becomes

$$\operatorname{Re} \{ z \} = \beta + \frac{1}{8\beta} - \frac{31}{384\beta^3} - .01 \quad (90)$$

The imaginary part of z in this case and all following ones is

$$\operatorname{Im} \{ z \} = .005 \quad (91)$$

When $\operatorname{Re} \{ f \}$ is negative, two starting points for each mode were chosen. This was necessary because of the presence of a saddle point in the region of each mode. One starting point is given by Eq. (90), with the proviso that it is shifted to the other side of $\operatorname{Re} \{ f \} = 0$, thus

$$\operatorname{Re} \{ z \} = \beta + \frac{1}{8\beta} - \frac{31}{384\beta^3} + .01 \quad (92)$$

TABLE 4

STARTING POINTS (EXCLUDING "STAND-OFF FACTOR")

s	Equations (90) and (92)	Equation (93)
	(v = 0)	(v = 1)
1	2.405	3.832
2	5.520	7.016
3	8.654	10.173
4	11.792	13.324
5	14.931	16.471
6	18.071	19.616
7	21.217	22.760
8	24.352	25.904
9	27.493	29.047
10	30.635	32.190
11	33.776	35.332
12	36.917	38.475
13	40.058	41.617
14	43.200	44.759
15	46.341	47.901
16	49.483	51.044
17	52.624	54.186
18	55.766	57.328
19	58.907	60.469
20	62.048	63.611

AD 1546 D

Eqs (89) and (91) apply.

The other starting point is also listed in Reference 3 and is given by

$$\operatorname{Re} \{ z \} = j_n + f_s - .01 \quad (93)$$

where $-.01$ is the "stand-off factor" and

$$f_s = \frac{1}{2} j_n \left[\frac{4K}{j_n^2 - 1} \right]^{1/2} \left[\frac{-5}{48K^2} + \frac{1}{K^{1/2}} \left(\frac{5}{24(j_n^2 - 1)^{3/2}} + \frac{1}{8(j_n^2 - 1)^{1/2}} \right) \right] \quad (94)$$

also

$$K = (2.25)^{1/3} \beta^{2/3} \quad (95)$$

with Eqs (89) and (91) applying.

The term j_n is found by iteration from

$$j_{n+1} = \frac{j_n}{\sqrt{j_n^2 - 1}} \left[\cos^{-1} \left(\frac{1}{j_n} \right) + \beta \right] \quad (96)$$

where j_{n+1} is the value of j_n after each iteration. The starting point for the iteration is

$$j_0 = 1.1 \quad (97)$$

Table 4 lists the first twenty starting points each for $\nu = 0$ (Eqs (90) and (92)) and for $\nu = 1$ (Eq. (93)). The data do not include the "stand-off factor". While the starting points are listed with respect to specific modes ($s-1$), this does not mean to imply that when one starts iteration from these starting points the listed modes are found. In some cases of interest the fundamental (zero) mode may only be found by an additional starting point. For large values of $\operatorname{Im} \{ z \}$, it can be shown by writing Eq. (54) in series of Bessel functions of real and of imaginary arguments that with

AD 1546 D



$$f = f_{\text{real}} + i f_{\text{imag}}$$

and

$$z = \alpha + i\beta$$

and

$$J_0(\alpha) = J_0(0) = 1$$

$$J_n(\alpha) = J_n(0) = 0$$

$$n = 1, 2, 3, \dots$$

$$f_{\text{real}} + i f_{\text{imag}} = (-\beta + i\alpha) \cdot \frac{I_1(\beta)}{I_0(\beta)}$$

when

$$\beta \rightarrow \infty$$

then

$$I_0 \rightarrow I_1$$

or

$$\text{Re } \{ z \} \rightarrow \text{Im } \{ f \}$$

and

$$\text{Im } \{ z \} \rightarrow -\text{Re } \{ f \}$$

} (98)

Equation (98) is used as an additional starting point when $\text{Re } \{ f \}$ is negative.

The solution of Eq. (57) is straight-forward. In fact, Table 4 gives the values of ak_r for the first 20 modes ($\nu = 1$). Higher modes ($s > 20$) may be found from Eq. (93), omitting the "stand-off factor".

AD 1545 D



Equations (61) and (64) may be solved by first finding a solution for $f_r = 0$, i.e., finding a solution as above (Eq. (87)), and then using this as the starting point in

$$z_{n+1} = z_n - \frac{F}{F'} \quad (99)$$

where, for Eq. (61) (inner and outer cylinders lined),

$$F = z_n f(q_o - r_o) + z_n^2 s_o - f^2 p_o \quad (100)$$

and

$$F' = z_n f(1-f_r)(p_o + s_o) - (z_n^2 + f^2 f_r) q_o - (z_n^2 f_r + f^2) r_o \quad (101)$$

A more efficient scheme is to find the starting points for Eq. (61) directly. With $f = 0$, Eq. (61) becomes

$$s_o = 0 \quad (102)$$

or

$$J_1(z)N_1(f_r z) - J_1(f_r z)N_1(z) = 0 \quad (103)$$

Ref. 3 can be used to find the starting points for any given value of f_r . The zeros of Eq. (103) are

$$\text{Re } \{ z \} = \frac{1}{f_r} \left\{ \beta + \frac{p}{\beta} + \frac{q-p^2}{\beta^3} + \frac{r-4pq+2p^3}{\beta^5} \right\} \quad (104)$$

where

$$\beta = \frac{s\pi}{\lambda-1}$$

$$p = \frac{\mu-1}{8\lambda}$$

$$q = \frac{(\mu-1)(\mu-25)(\lambda^3-1)}{6(4\lambda)^3(\lambda-1)}$$

AD 1545 D



$$r = \frac{(\mu - 1)(\mu^2 - 114\mu + 1073)(\lambda^5 - 1)}{5(4\lambda)^5(\lambda - 1)}$$

$$\lambda = \frac{1}{f_r}$$

$$\mu = 4$$

$$s = 1, 2, 3, \dots, N$$

When f_r is about .8 or larger, the last term on the right in Eq. (104) can be dropped.

When $\text{Re } \{ f \}$ is positive, subtract a stand-off factor from the right side of Eq. (104); if negative, add a stand-off factor. The stand-off factor is .01 in both cases.

Another zero of Eq. (61) for $\text{Re } \{ f \}$ negative can be found for $f = \infty$. Substituting this value for f into Eq. (61) results in

$$p_0 = 0 \tag{106}$$

or

$$J_0(z)N_0(f_r z) - J_0(f_r z)N_0(z) = 0 \tag{107}$$

Eqs (104) and (105) hold, except that now

$$\mu = 0 \tag{108}$$

Subtract the stand-off factor from the right side of Eq. (104). Eqs (99) to (101) are applicable.

Also, for $\text{Re } \{ f \}$ negative, Eq. (98) must be used as a starting point. In the following cases it is understood that Eq. (98) is

always used as an additional starting point. For any given engine model (f_r fixed), the starting points are calculated only once and thereafter can be programmed in the form of tables. The same holds for starting points in the following sections.

For the solution of Eq. (64) (outer cylinder wall only lined) one has in Eq. (99)

$$F = f + z_n \frac{s_o}{q_o} \quad (109)$$

$$F' = -z_n \left\{ 1 + \frac{1}{q_o} \left[f_r r_o - \frac{s_o}{q_o} (f_r p_o - s_o) \right] \right\} \quad (110)$$

The starting points for the iterative solution of Eq. (64) are found from $f = 0$:

$$s_o = 0 \quad (111)$$

Eqs (104) and (105) are used with a stand-off factor .01 subtracted from the right side of Eq. (104) for $\text{Re} \{ f \}$ positive and added for $\text{Re} \{ f \}$ negative. An additional zero of Eq. (64) for $\text{Re} \{ f \}$ negative is found for $f = i\infty$. Substitution in Eq. (64) yields

$$q_o = 0 \quad (112)$$

or

$$J'_o(f_r z) N_o(z) - J_o(z) N'_o(f_r z) = 0 \quad (113)$$

Eq. (104) applies, but

$$\beta = \frac{(s - \frac{1}{2})\pi}{\lambda - 1}$$

$$p = \frac{(\mu + 3)\lambda - (\mu - 1)}{8\lambda(\lambda - 1)} \quad (114)$$

$$q = \frac{(\mu^2 + 46\mu - 63)\lambda^3 - (\mu - 1)(\mu - 25)}{6(4\lambda)^3(\lambda - 1)}$$



$$r = \frac{(\mu^3 + 185\mu^2 - 2053\mu + 1899)\lambda^5 - (\mu - 1)(\mu^2 - 114\mu + 1073)}{5(4\lambda)^5 (\lambda - 1)}$$

$$\lambda = \frac{1}{f_r}$$

$$\mu = 0$$

$$s = 1, 2, 3, \dots, N$$

Subtract the stand-off factor from the right side of Eq. (104).

For the solution of Eq. (66) (inner cylinder wall only lined) the substitutions in Eq. (99) are

$$F = f - z_n \frac{s_o}{r_o} \quad (115)$$

$$F' = z_n \left\{ f_r + \frac{1}{r_o} \left[q_o - \frac{s_o}{r_o} (p_o - f_r s_o) \right] \right\} \quad (116)$$

One set of starting points is obtained from Eqs (104) and (105). The other for $\text{Re} \{f\}$ negative is obtained from $f = i\infty$, or

$$r_o = 0 \quad (117)$$

$$J_o(f_r z) N'_o(z) - J'_o(z) N_o(f_r z) = 0 \quad (118)$$

Eqs (104) and (114) apply, except that the right side of Eq. (104)

is multiplied by f_r , and in Eq. (114) $\lambda = f_r$.

Equation (69) (no lining) is solved directly from Eqs (104) and (105).

No stand-off factor is used.

Equation (71) may be solved by substitution into Eq. (99) of

$$F = f - z_n \frac{J_{m+1}(z_n)}{J_m(z_n)} \quad (119)$$



$$F' = 2m \frac{J_{m+1}(z_n)}{J_m(z_n)} - z_n \left(1 + \frac{J_{m+1}^2(z_n)}{J_m^2(z_n)} \right) \quad (120)$$

where

$$f = ia(k + m)$$

$$m = 0, 1, 2, 3, \dots \quad (121)$$

$$z_n = ak_r$$

The starting points may be taken from Table 4 and 5 with $2' = m$. The listed values are starting values for $\text{Re} \{ z_n \}$. (A "stand-off factor" must be added).

When $\text{Re} \{ f \}$ is positive, the "stand-off factor" is (-.01). $\text{Im} \{ z \}$ is (+.005). $s = 1, 2, 3, \dots, N$ where N is the number of modes required. The table lists only values of $\text{Re} \{ z \}$ for m from 0 to 8. Additional values may be found from the following procedure:

$$\text{Re} \{ z \} = mj_n + \frac{f_s}{m} - .01 \quad (122)$$

where

$$f_s = \frac{1}{2} j_n \left[\frac{4K}{j_n^2 - 1} \right]^{1/2} \left[\frac{-5}{48K^2} + \frac{1}{K^{1/2}} \left(\frac{5}{24(j_n^2 - 1)^{3/2}} + \frac{1}{8(j_n^2 - 1)^{1/2}} \right) \right] \dots \quad (123)$$

also,

$$K = (2.25)^{1/3} \left(\frac{\beta}{m} \right)^{2/3} \left[1 + \frac{5}{108} \frac{1}{\beta^2} \right] \quad (124)$$

TABLE 5
STARTING POINTS (EXCLUDING "STAND-OFF FACTOR")

<u>s</u>	<u>v = 2</u>	<u>v = 3</u>	<u>v = 4</u>	<u>v = 5</u>	<u>v = 6</u>	<u>v = 7</u>	<u>v = 8</u>
1	5.136	6.380	7.588	8.771	9.936	11.086	12.225
2	8.417	9.761	11.065	12.339	13.589	14.821	16.038
3	11.620	13.015	14.373	15.700	17.004	18.288	19.555
4	14.796	16.223	17.616	18.980	20.321	21.642	22.945
5	17.960	19.409	20.827	22.218	23.586	24.935	26.267
6	21.117	22.583	24.019	25.430	26.820	28.191	29.546
7	24.270	25.748	27.199	28.267	30.034	31.423	32.796
8	27.421	28.908	30.371	31.812	33.233	34.637	36.026
9	30.569	32.065	33.537	34.989	36.422	37.839	39.240
10	33.717	35.219	36.699	38.160	39.603	41.031	42.444
11	36.863	38.370	39.858	41.326	42.778	44.215	45.638
12	40.008	41.521	43.014	44.489	45.949	47.394	48.826
13	43.153	44.670	46.168	47.649	49.116	50.568	52.008
14	46.298	47.818	49.320	50.807	52.279	53.738	55.185
15	49.442	50.965	52.472	53.963	55.441	56.905	58.358
16	52.586	54.112	55.622	57.117	58.600	60.069	61.528
17	55.730	57.258	58.771	60.270	61.757	63.231	64.695
18	58.873	60.403	61.919	63.422	64.913	66.391	67.859
19	62.016	63.548	65.067	66.573	68.067	69.550	71.022
20	65.159	66.693	68.214	69.723	71.220	72.707	74.183

AD 1546 D



and, using an iteration method to find j_n :

$$j_{n+1} = \frac{j_n}{\sqrt{j_n^2 - 1}} \left[\cos^{-1} \left(\frac{1}{j_n} \right) + \frac{2}{3} K^{3/2} \right] \quad (125)$$

β is obtained from Eq. (89). The starting point for Eq. (125) is $j_0 = 1.1$. The "stand-off factor" is included in Eq. (122).

When $\text{Re} \{ f \}$ is negative, the "stand-off factor" applied to tabulated values (Table 4 and 5) is (+.01) for $\mathcal{V} = m$. The additional starting points required are obtained from Table 4 and 5 with $\mathcal{V} = m + 1$ and a "stand-off factor" of (-.01). To extend the table beyond $m = 8$ and/or $s = 20$, the above procedure may be adopted. For the first set of starting points the third term on the right of Eq. (122) is replaced by (+.01). The second set of starting points is obtained by replacing (m) with (m+1) in Eqs (122) through (125).

The solution of Eq. (72) is relatively simple. Since m is a real number, ak_r is also a real number. Also, since m is a positive number, the iteration to solve Eq. (72) starts with Eqs (122) through (125), and

$$\text{Im} \{ z \} = 0 \quad (126)$$

Tables 4 and 5 may be utilized instead, provided a "stand-off factor" of (-.01) is used.

The equation to be solved by iteration is

$$z_{n+1} = z_n + \frac{m - z_n \frac{J_{m+1}(z_n)}{J_m(z_n)}}{z_n \left[1 + \left(\frac{J_{m+1}(z_n)}{J_m(z_n)} \right)^2 \right] - 2m \frac{J_{m+1}(z_n)}{J_m(z_n)}} \quad (127)$$

Equation (74) is solved by setting G equal to zero:

$$ibk\ell = -f_r m \quad (128)$$

and

$$H_{p_{m+1}} + D t_{m+1,m} = 0 \quad (129)$$

or

$$f_r z p_{m+1} - m(1 + f_r) t_{m+1,m} = 0 \quad (130)$$

where z is taken as a real number. One method of finding the zeros of Eq. (130) is to solve Eq. (130) for increasing values of z ($z = .001, 1, 2, 3, \dots$) until a z is reached for which the left side of Eq. (130) changes sign. Then this value of z is used as a starting point in the tangent method. Calling the left side of Eq. (130) F and differentiating F with respect to z yields

$$F' = \left[z f_r^2 + \frac{m(1 + f_r)}{z} \right] t_{m+1,m} + z f_r t_{m,m+1} - \left[(1 + f_r) m p_m + f_r (1 + m(1 - f_r)) p_{m+1} \right] \quad (131)$$

Substituting F and F' into Eq. (99) yields z . The solution of Eq. (74) may now be found by iteration of Eq. (99) where F is defined by Eq. (132) and F' defined by Eq. (133). The starting

point when $\text{Re} \{ C \}$ is negative is the complex number ($z = .01, .005$).

$$F = CD p_m - GH p_{m+1} + CH t_{m,m+1} - DG t_{m+1,m} \quad (132)$$

and

$$F' = \frac{1}{G} [D(2Gm - G^2) + CH^2] p_m + H [D - C + 2m] p_{m+1} - [CD + H^2] t_{m+1,m} - f_r [CD + G^2] t_{m,m+1} \quad (133)$$

As before, this may not yield all modes, therefore another starting point is obtained from $C = \infty$: or

$$F = p_m = 0 \quad (134)$$

Eqs (104) and (105) can be used to find $\text{Re} \{ z \}$, with the provision that $\mu = 4m^2$. $z = \text{Re} \{ z \}$ yields the starting point in Eqs (99), (132), and (133) for $\text{Re} \{ C \}$ negative: ($\text{Re} \{ z \} + .01, .005$) and for $\text{Re} \{ C \}$ positive: ($\text{Re} \{ z \} - .01, .005$).

Equation (75) is solved similarly, except that D in Eqs (132) and (133) is set equal to $(-m)$. Equation (130) becomes

$$F = f_r z p_{m+1} - m t_{m+1,m} = 0 \quad (135)$$

and Eq. (131) is

$$F' = \left[z f_r^2 + \frac{m}{z} \right] t_{m+1,m} + z f_r t_{m,m+1} - \left[m p_m + f_r (1 + m) p_{m+1} \right] \quad (136)$$

The other starting point (equivalent to Eq. (134)) is found from

$C = \infty$, or

$$F = m p_m - f_r z t_{m,m+1} \quad (137)$$

$$F' = \left(2 \frac{m^2}{z} - f_r^2 z \right) p_m + f_r z p_{m+1} - m [t_{m+1,m} + f_r t_{m,m+1}] \quad (138)$$

Equation (76) is solved by first solving Eq. (72) and using the result (with $C = m$ and $D = -m$) as a starting point in Eqs (99) (132), and (133).

Equation (77) is again solved similarly to Eq. (74). Setting D equal to zero, and with z a real number:

$$F = m t_{m,m+1} - z p_{m+1} \quad (139)$$

and

$$F' = m f_r p_m + (m+1) p_{m+1} - (z + \frac{m}{z}) t_{m,m+1} - z f_r t_{m+1,m} \quad \dots(140)$$

This yields the starting points for Eqs (132) and (133), where now $C = m$. Equation (139) is solved and used like Eq. (130). With $D = \infty$ the other starting points are found:

$$F = m p_m - z t_{m+1,m} \quad (141)$$

$$F' = (\frac{2m^2}{z} - z) p_m + f_r z p_{m+1} - m (f_r t_{m,m+1} + t_{m+1,m}) \quad (142)$$

Equation (141) is solved like Eq. (129) and the results are used like Eq. (134).

For annular ducts with struts the solution of the wave equation is similar to that for annular ducts with asymmetric pressure distribution. The only difference is that in the former the permissible values of m are restricted by Eq. (85),

AD 1546 D

The solution of the equations for k_r in ducts with other than still air can be found by finding k_r first for $M = 0$, and then using this solution as a starting point in the iterative solution of the same equations modified by the use of Eqs (85d) and (85e) and finding k_z from Eq. (85c)

In Table 6, the procedures for the numerical solution of all cylindrical and annular duct lining problems discussed are summarized.



TABLE 6
SUMMARY OF SOLUTION TECHNIQUE
CYLINDRICAL AND ANNULAR DUCTS

	a	b	c	d
TYPE LINING	CYLINDRICAL DUCTS AXISYMM. PRESS. DISTR. (LINED)	SAME, NO LINING	ANNULAR DUCTS AXISYMM. PRESS. DISTR. (LINED)	SAME, LINING ON INTERIOR OF OUTER WALL ONLY
SOLVE	54	57	61	64
USING	87	Table 3 or 89, 93 (without "stand-off factor"), 94-97	99-101	99, 109, 110
WITH STARTING POINTS	Table 4 or for $\text{Re} \{ f \} \geq 0$: 89-91 for $\text{Re} \{ f \} < 0$: 89, 91, 92 89, 91, 94-97 98		for $\text{Re} \{ f \} \geq 0$: 103-105 for $\text{Re} \{ f \} < 0$: 103-108, 98	for $\text{Re} \{ f \} \geq 0$: 103-105 for $\text{Re} \{ f \} < 0$: 103-105, 113-114, 98

TABLE 6 (continued)

TYPE LINING	e SAME, LINING ON EXTERIOR WALL OF INNER CYL. ONLY	f SAME, NO WALLS LINED	g CYL. DUCT WITH ASYM. PRESS. DISTR. (LINED)	h SAME, NO LINING
SOLVE	66	69	71	72
USING	99, 115, 116	104, 105 (no 'stand- off' factor.)	99, 119, 120	127

WITH
STARTING
POINTS

for $\text{Re } \{f\} \geq 0$:
103-105

for $\text{Re } \{f\} < 0$:
103-105, 114, 118, 98
(check on changes in
Eqs (104) and (114))

Tables 4 and 5
($\mathcal{V} = m$ for $\text{Re } \{f\} \geq 0$;
 $\mathcal{V} = m$ & $\mathcal{V} = m+1$
for $\text{Re } \{f\} < 0$)
or
89, 122-125
98

Table 4 and 5
($\mathcal{V} = m$) or
89, 122-126

TABLE 6 (continued)

l

i

j

k

ANNULAR DUCTS
ASYMM. PRESS.
DISTR. (LINED)

SAME, LINING
ON INTERIOR OF
OUTER WALL ONLY

SAME, LINING
ON EXTERIOR
OF INNER WALL ONLY

SAME, NO
LINING

SOLVE

74

75

77

76

USING

99, 132, 133

99, 132, 133
(with $D = -m$)

99, 132, 133
(with $C = m$)

Solution of 72

WITH
STARTING
POINTS

for $\text{Re } \{C\} \geq 0$:
134
for $\text{Re } \{C\} < 0$:
99, 130, 131,
134, 98

for $\text{Re } \{C\} \geq 0$:
99, 137, 138
for $\text{Re } \{C\} < 0$:
99, 135-138, 98

for $\text{Re } \{D\} \geq 0$:
99, 141, 142
for $\text{Re } \{D\} < 0$:
99, 139-142, 98

See Column (h)
Substitute
results in
99, 132, 133
($C = m, D = -m$)

TABLE 6 (continued)

m	n	o	p
ANNULAR DUCTS WITH STRUTS (CYL. WALLS LINED)	SAME, LINING ON INTERIOR OF OUTER WALL ONLY	SAME, LINING ON EXTERIOR OF INNER WALL ONLY	SAME, NO LINING
SOLVE	74, 85, or 85b	75, 85, or 85b	77, 85, or 85b
USING	Solution of 74	Solution of 75	Solution of 76
WITH STARTING POINTS	See Column (i) Note: Values of m selected according to 85 or 85b	See Column (j) See note in Column (m)	See Column (k) See note in Column (m)



2.4 SOUND ATTENUATION IN CURVED RECTANGULAR DUCTS

In a rectangular duct with constant curvature the wave propagation is taken in the φ -direction. The z-axis passes through the center of curvature and is perpendicular to the plane of the duct centerline.

2.4.1 Solution of the Wave Equation

Equation (43) applies and has the solution

$$p = \left[AJ_m(k_r r) + BN_m(k_r r) \right] \left[C \cos(k_z z) + S \sin(k_z z) \right] e^{i(\omega t - m \varphi)} \quad (143)$$

where

$$k = \sqrt{k_r^2 + k_z^2} = \frac{\omega}{c} \quad (144)$$

k_r , k_z and m can be determined from the boundary conditions.

2.4.2 Boundary Conditions

Assuming that all walls are lined, the boundary conditions lead to the following equations. If the lining at $r = a$ has a normalized admittance l_a , then the particle velocity normal to this wall is

$$\begin{aligned} v_n &= -\frac{1}{i\omega\xi} \left(\frac{\partial p}{\partial r} \right)_{r=a} \\ &= \frac{l_a}{\xi c} p_{r=a} \end{aligned} \quad (145)$$

or

$$\frac{kl_a}{ik_r} = \frac{AJ'_m(k_r a) + BN'_m(k_r a)}{AJ_m(k_r a) + BN_m(k_r a)} \quad (146)$$

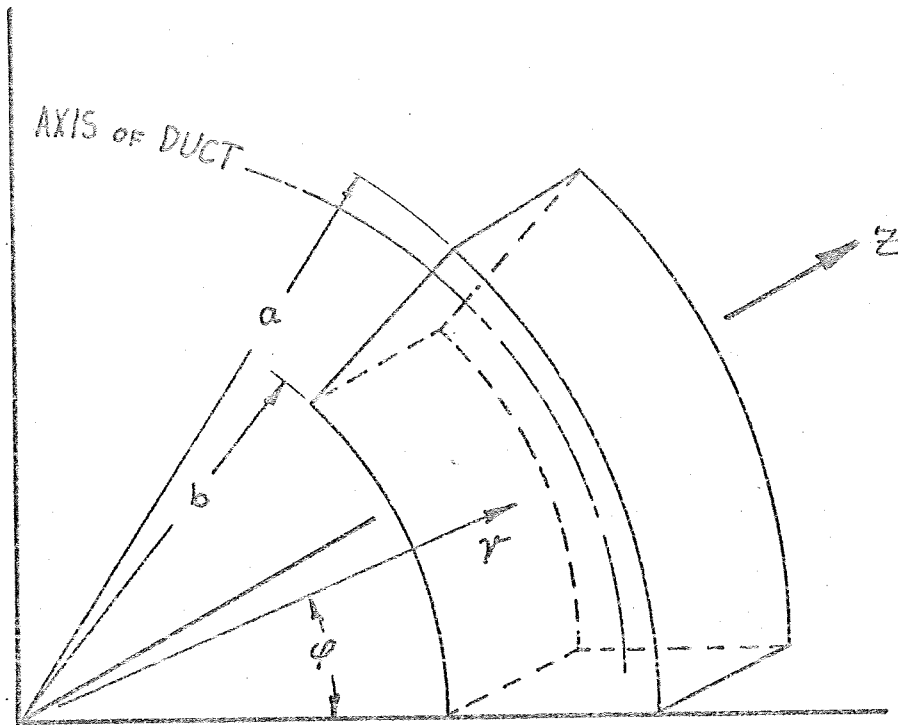


Fig. 8

Coordinate System for Curved Duct

AD 1546 D



where the primes indicate differentiation with respect to (k_r) .

If the lining at $r = b$ has a normalized admittance l_b , then the particle velocity normal to this wall is

$$\begin{aligned} v_n &= \frac{1}{i\omega\xi} \left(\frac{\partial p}{\partial r} \right)_{r=b} \\ &= \frac{l_b}{\xi c} p_{r=b} \end{aligned} \quad (147)$$

or

$$\frac{k l_b}{i k_r} = - \frac{AJ'_m(k_r b) + BN'_m(k_r b)}{AJ_m(k_r b) + BN_m(k_r b)} \quad (148)$$

If the lining at $z = 0$ has a normalized admittance l_o , then, equivalent to the above,

$$\frac{k l_o}{i k_z} = - \frac{S}{C} \quad (149)$$

of the lining at $z = g$ has a normalized admittance l_g , then

$$\frac{k l_g}{i k_z} = \frac{-C \sin(k_z g) + S \cos(k_z g)}{C \cos(k_z g) + S \sin(k_z g)} \quad (150)$$

Equations (149) and (150) are combined by eliminating $\frac{S}{C}$:

$$\left[\frac{k^2 l_o l_g}{k_z} + k_z \right] \tan(k_z g) - ik(l_o + l_g) = 0 \quad (151)$$

This equation is of the same form as Eq. (24), and can be solved for k_z . k_r is found using Eq. (144) and is substituted into Eqs (146) and (148) after elimination of $\frac{A}{B}$:

$$f_a f_b p_m + f_a f_b q_m - f_b f_r m - s_m = 0 \quad (152)$$



where

$$\begin{aligned}
 f_a &= \frac{k \ell_a}{ik_r} \\
 f_b &= \frac{k \ell_b}{ik_r} \\
 p_m &= J_m(ak_r)N_m(bk_r) - J_m(bk_r)N_m(ak_r) \\
 q_m &= J_m(ak_r)N'_m(bk_r) - J'_m(bk_r)N_m(ak_r) \\
 r_m &= J'_m(ak_r)N_m(bk_r) - J_m(bk_r)N'_m(ak_r) \\
 s_m &= J'_m(ak_r)N'_m(bk_r) - J'_m(bk_r)N'_m(ak_r)
 \end{aligned}
 \tag{153}$$

Methods similar to those outlined in Section 2.3.3 may be used to solve Eq. (152) for m .

The attenuation per unit length of duct is

$$D = 8.68 \times \frac{1}{r_{ab}} \times \text{Im} \{ m \}
 \tag{154}$$

where r_{ab} is the radius of curvature of the centerline of the duct

$$r_{ab} = \frac{1}{2} (a + b)
 \tag{155}$$

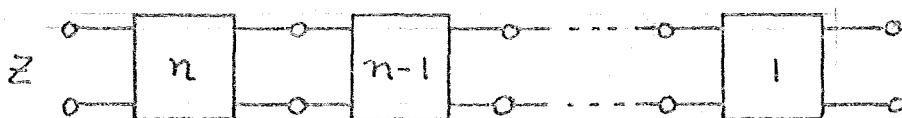
AD 1546 D



2.5 LINING IMPEDANCE

A lining is built up from a number of layers, which are parallel to the duct wall. These layers can simply be air spaces, or they can be dissipative layers of porous material. If the lining is "locally reacting", its effect on acoustic waves is completely described by its "normal incidence impedance". A lining is locally reacting when it is divided into compartments, which are perpendicular to the duct wall. Such compartments prevent waves from traveling inside the lining in directions other than those normal to the duct wall. The analysis will be limited to locally reacting linings.

The impedance of a multi-layer lining is calculated using electrical analogies. Each layer in the lining is regarded as a four-pole, and the total lining will thus be a cascade of four-poles.

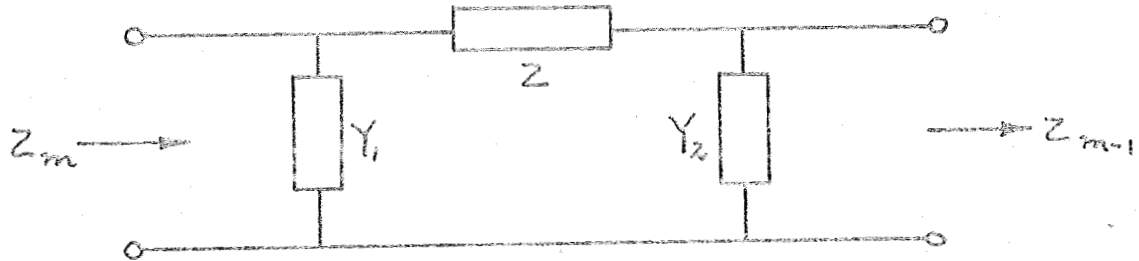


The input impedance of this cascade is the lining impedance. The output of four-pole No. 1 is open, indicating that the layer closest to the duct wall is terminated by an infinite impedance, viz. that of the rigid wall.

Two types of four-poles are considered, corresponding to two different types of layers, "discrete element type" and "continuous element type".

2.5.1 Discrete Element Type

This type is characterized by three elements in a π -link configuration. For convenience, the two shunting elements of this configuration are given by their admittances rather than their impedances, since, in the limiting case when the layer is thin, these admittances are zero.



The input impedance of the link is denoted by Z_m , and the input impedance of the preceding link, which constitutes the load impedance on the output of link number m , is denoted by Z_{m-1} . The use of input and output admittances instead of impedances leads to somewhat shorter expressions, thus for the input admittance we get:

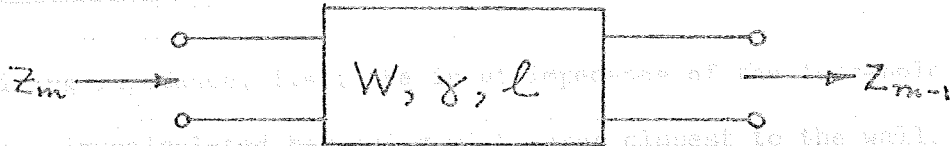
$$Y_m = Y_1 + \frac{1}{Z + \frac{1}{Y_2 + Y_{m-1}}} \quad (156)$$

In the case of hard termination, as for $m = 1$, $Y_{m-1} = 0$.

The values of Y_1 , Z , Y_2 , which in general are all complex numbers, can be determined theoretically or experimentally. A computer program for evaluation of Z from measurements performed in an impedance tube on thin layers (for which $Y_1 = Y_2 = 0$) is described in Ref. 4.

2.5.2 Continuous Element Type

This type corresponds to an electrical transmission line, and is characterized by its characteristic impedance W , its propagation constant γ , and its length l (= thickness of the layer).



The input impedance Z_m of a transmission line terminated by an impedance Z_{m-1} is (cf. ref. 5):

$$Z_m = W \frac{Z_{m-1} \cosh \gamma l + W \sinh \gamma l}{Z_{m-1} \sinh \gamma l + W \cosh \gamma l} \quad (157)$$

Rewriting this expression in the more convenient admittance form we get

$$Y_m = \frac{1}{W} \frac{W Y_{m-1} - i \tan(\gamma l)}{1 - i W Y_{m-1} \tan(\gamma l)} \quad (158)$$

W and γ are theoretically or experimentally determined values. W is a real number and γ are in general complex numbers. For γ we have

$$\gamma = \alpha + i\beta \quad (159)$$

where α is the attenuation constant and β is the phase constant. β is given by

$$\beta = \omega/c_m = 2\pi f/c_m \quad (160)$$

where c_m is the speed of sound in the material.

An air space is a special case of the continuous type layer, viz.

$\alpha = 0$, $c_m = c$, and $W = 1$.

2.5.3 Composite Lining

The lining impedance, i.e., the input impedance of the four-pole cascade, is calculated beginning with layer closest to the wall, since the output admittance of the wall, $Y_o = 0$, is known. Equation (158) for the air space next to the rigid wall becomes

$$Y = -i \tan(i\gamma \ell_1) \quad (161)$$

The pervious material next to this air space changes the input admittance to that given by Eq. (156), where Y_{m-1} is given by Eq. (161). Equations (156) and (158) are used alternately to find the input admittance of a composite lining.



2.6 TOTAL ATTENUATION

The attenuation of the waves along the duct is given by the form of the function describing the amplitude variation with the coordinate in the direction of propagation. This is the z-direction in Sections 2.2 - 2.3, and the φ -direction in Section 2.4. From Section 2.2.1 we get for the first case

$$p \sim z = e^{-ik_z z} \quad (162)$$

or

$$p \sim e^{-iz\text{Re}\{k_z\}} e^{z\text{Im}(k_z)} \quad (163)$$

The attenuation D per unit length of the duct, in dB measure, is given by

$$\begin{aligned} D &= 20 \log_{10} \frac{|p(z=z_0)|}{|p(z=z_0+1)|} = 20 \log_{10} e^{-\text{Im}(k_z)} = \\ &= -8.68 \text{Im}(k_z) \dots \end{aligned} \quad (164)$$

Equation (11) for k_z has two solutions differing from each other by a sign. We must choose the solution that gives a wave of decreasing amplitude along the propagation path, and therefore we can rewrite Eq. (164)

$$D = 8.68 | \text{Im}(k_z) | \quad (165)$$

For the case described in Section 2.4 we get analogously

$$D = 8.68 \frac{| \text{Im}(m) |}{r_m} \quad (166)$$

where r_m is some arbitrarily defined mean radius of the curved duct.

The general solution of the wave equation in the duct is a superposition of all solutions of the type given in Eq. (10a). Each of Eqs (13) and (14) for k_x and k_y has an infinite number of solutions. Let us number the solutions $m = 0, 1, 2, \dots$ and $n = 0, 1, 2, \dots$, respectively. Each pair (m, n) thus corresponds to a solution of k_z , Eq. (11), and will be referred to as a "mode". The attenuations, D_{mn} , for the different modes are thus different. Assume that the energy in mode (m, n) at the entry of the duct is $E_{mn}(0)$. Then the energy in that mode a distance z from the entry is

$$E_{mn}(z) = E_{mn}(0) 10^{-D_{mn} z/10} \quad (167)$$

For the total energy, made up from all modes, we can write

$$E(z) = \sum_{m,n} E_{mn}(z) = \sum_{m,n} E_{mn}(0) 10^{-D_{mn} z/10} \quad (168)$$

The total attenuation for a duct of length L can thus be written

$$D_L = 10 \log_{10} \frac{E(0)}{E(L)} = 10 \log_{10} \frac{\sum_{m,n} E_{mn}(0)}{\sum_{m,n} E_{mn}(0) 10^{-D_{mn} L/10}} \quad \dots \quad (169)$$

The attenuation is, for practical purposes, best described by an insertion loss, i.e., the difference in attenuation between a lined and an unlined duct

$$IL = D_L - D'_L = 10 \log_{10} \frac{\sum_{m,n} E_{mn}(0) 10^{-D'_{mn}L/10}}{\sum_{m,n} E_{mn}(0) 10^{-D_{mn}L/10}} \quad (170)$$

where the primes refer to the unlined duct. The value of IL is not sensitive to the number of modes included, as long as this number is sufficiently large.

The number of modes to be included can be estimated from Eqs (16) and (17). For the unlined duct k_x and k_y are real for all modes, as can be seen from Eq. (16). Thus only modes for which

$$k_x^2 + k_y^2 > k^2 \quad (171)$$

will be attenuated, cf Eq. (17). The attenuation of modes, for which Eq. (171) holds with some margin, is, however, very large, and these modes do not have to be included in the summation.

This gives maximal values of m and n , which can be calculated from Eq. (16) and the corresponding expression for k_x .

2.7 SUBJECTIVE NOISE AND MERIT FUNCTION

The effectiveness of a lining, as applied to an aircraft, should be judged from the difference in annoyance on the ground at flyovers of aircrafts with lined and with unlined ducts. As a measure of the annoyance the "perceived noise level" (PNL) is used. It is a value calculated from a sound spectrum in the following manner:

The spectrum is given as a number of sound pressure levels L_i for frequency bands i . From these levels, the octave band levels O_j are calculated for standard octave bands j , given in Ref. 6. We have

$$O_j = 10 \log_{10} \sum_i 10^{L_i/10} \quad (172)$$

where the summation should be carried out over all i 's corresponding to frequencies within band j (obvious adjustments have to be made for an interval i that falls in two different intervals j). The levels O_j correspond, conventionally, to "noisiness" values N_j according to tables given in Ref. 6. The perceived noise level is then defined as

$$PNL = 40 + 33.3 \log_{10} (0.7 N_m + 0.3 \sum_j N_j) \quad (173)$$

where N_m is the maximal value of all N_j . A standard subroutine that calculates PNL from L_i 's is available.

Of the total sound from an aircraft, only a part propagates through the lined duct and hence is subject to attenuation. Therefore, the

sound spectrum at the chosen ground position is divided into two spectra, one affected by the presence of a lining, and one unaffected. Let the levels in the different frequency bands of the former be A_i , and of the latter be B_i (given). We have

$$L_i = 10 \log_{10} (10^{A_i/10} + 10^{B_i/10}) \quad (174)$$

Let the given (usually measured) sound spectrum levels at the ground position for an aircraft with unlined duct be A_i' . Then the levels A_i are calculated using Eq. (170) for IL

$$A_i = A_i' - IL \quad (175)$$

Now PNL can be calculated using Eqs (172)-(175). PNL is taken to be the merit function which is going to be minimized. In the optimization procedure, the values of lining parameters are varied until a minimum in PNL is reached. The parameters giving minimum PNL, are optimal in the sense that when used in the design of linings for an aircraft, this aircraft will give minimum annoyance at flyover, when fitted with linings.



2.8 OPTIMIZATION PROGRAM

The subroutine MINUM is used for the optimization procedure. The algorithm for MINUM is described in Ref. 1. Only an excerpt of the reference paper is given here.

MINUM determines the minimum value of a function of several variables. The function may have discontinuities, many relative minima and need not be differentiable.

The minimum value of the function is found by a comparative evaluation of the function for many values of the normalized variables. The following four methods are used to change the values of the variables.

- (1) Gradient steps
- (2) Random direction steps. If unsuccessful, a step is taken in the opposite direction.
- (3) Average direction step (the direction for this step is the average of the previous five successful steps)
- (4) Random jump step

In the first three methods, the step size is dependent upon the number of successes and failures in previous steps. The rate at which each method is used can be specified by the user.

Two other methods to change the variables are used when the previous step was near a boundary. These are the mirrored step and the boundary gradient step.



While it is always preferable to continue the MINUM iteration until the value of the function is that of the global optimum, it is seldom practical to do so (excess computer time). In most cases, however, there are a multitude of local minima, many of which will give values of the function meeting design requirements.

AD 1543 D



REFERENCES

1. The Boeing Company, Commercial Airplane Division, SAAC Documentation Center, Subroutine MLNUM, 1966.
2. "Die Grundlagen der Akustik", E. Skudrzyk, Springer Verlag, 1954.
3. Handbook of Mathematical Functions, Applied Mathematics Series 55, (June 1964).
4. Boeing Company, D6-29276TN, "Calculation of Acoustical Impedance from Impedance Tube Measurements", Reddaway, A.R.F., 19 July 1967, Transport Division.
5. "Fundamentals of Acoustics", Frey, A. R. and Kinsler, L. E., Wiley, 1962.
6. "Noise Reduction", Beranek, L. L., McGraw-Hill, 1960
7. Boeing Company, D6-29560TN, "Prediction and Optimization of Sound Attenuation in Lined Rectangular Ducts with Computer Programs", J. S. Westall, 1968, Transport Division.
8. Boeing Company, D6-29745TN, "Prediction of Sound Attenuation in Lined Annular Ducts with Computer Programs", J. S. Westall, to be released 1968-69, Transport Division.

